

Chapter 5

IN VIVO DIAGNOSTICS AND METRICS IN THE ASSESSMENT OF LASER-INDUCED RETINAL INJURY

HARRY ZWICK, PhD^{*}; JAMES W. NESS, PhD[†]; MICHAEL BELKIN, MD[‡]; AND BRUCE E. STUCK, MS[§]

INTRODUCTION

VISUAL FUNCTION: SHIFTING FOCUS BEYOND THE MACULA

ASSESSING IN VIVO RETINAL MORPHOLOGY

Confocal Scanning Laser Ophthalmoscopy
Optical Coherence Tomography

FUNCTIONAL METRICS AND STRUCTURAL CORRELATES

Assessing Visual Function Along the Visual Pathway
Integrating Imaging With Visual Function

LASER ACCIDENT CASES

Case 1
Case 2
Case 3
Case 4
Case 5

REVIEW

SUMMARY

^{*}Formerly, Team Leader, Retinal Assessment Team, US Army Medical Research Detachment, Brooks City-Base, San Antonio, Texas 78235-5108; currently retired

[†]Colonel, Medical Service Corps, US Army; Program Director, Engineering Psychology, Department of Behavioral Sciences and Leadership, US Military Academy, West Point, New York 10996

[‡]Goldschleger Eye Research Institute, Sheba Medical Center, Tel Aviv University, Tel Hashomer 52621, Israel

[§]Director, Ocular Trauma Research Division, US Army Institute of Surgical Research, 3400 Rawley East Chambers Avenue, San Antonio, Texas 78234-6315; currently retired

INTRODUCTION

The field of laser–tissue interactions encompasses almost all branches of science, including basic and applied physics, engineering, meteorology, biology, and medicine. Since the invention of lasers in the middle of the last century, lasers have become ubiquitous, and the study of laser bioeffects has employed the talents and expertise of many scientists, engineers, and physicians around the world. The history of the invention and development of the laser and its multitude of applications is well known. It is a saga of almost unmitigated success in basic and applied research.

The US military’s interest and involvement in laser bioeffects began soon after the laser was first invented in 1960. As the military began to investigate and use laser instruments at wavelengths potentially injurious to the human eye, it realized the need to study the extent of this new potential hazard. Many of the most notable achievements in the field of laser safety research can be traced directly to the original work of Colonel Edwin S Beatrice, MD, and his interdisciplinary team of Army scientists, physicians, and engineers who devoted their careers to the gathering of data necessary to formulate safety standards and procedures. Dr Beatrice’s original scientific approach to determining the safety of laser beam characteristics in the 1970s was later applied to the United States and international standards for the safe use of all lasers.

The US Army established the US Army Medical Research and Development Command and the US Army Materiel Command Joint Laser Safety Team

in 1968 at the Frankford Arsenal in Philadelphia, Pennsylvania. The purpose of the Army’s laser safety program was to support development of military lasers by minimizing their potential risks to soldiers in the field. The laser safety research team was a group of highly dedicated investigators who worked at the forefront of all relevant scientific disciplines, including physics, histopathology, psychophysics, and medicine. The history of the research from its inception in 1968 to its discontinuation in 2011 is summarized in Exhibit 5-1. This chapter describes an approach to researching laser-induced changes to visual function, focusing on relating retinal structural changes, anomalies, and damage to changes in visual function based on the accumulated experience of the laser safety research team.

Worldwide today, military laser systems are known to be in use by 49 nations. Military lasers are used to support a wide variety of battlefield needs, including range-finding, communication, illumination, landmine and bomb detection and detonation, target designation, and detection of contamination. All are potentially hazardous to the human eye at tactical ranges. Although prophylactic and protective measures have been eminently successful in limiting the numbers of laser-induced injuries in the medical, laboratory, and industrial environments, these same measures are not easily applied in combat. In fact, the problem of protecting military combatants against laser-induced injury is exceedingly difficult.

VISUAL FUNCTION: SHIFTING FOCUS BEYOND THE MACULA

Laser-induced retinal injury is a function of both the nature of the laser exposure and the retina’s acute and long-term response to the exposure. In conventional classifications of laser-induced retinal damage, classification is based on acute laser-induced central retinal injury,¹ with little attention given to the manifestation of secondary functional abnormalities as the effects of the acute damage diminishes. Together with the application of well-targeted functional assessment, advanced imaging techniques have enhanced the understanding of laser-induced retinal sequelae.² Exhibit 5-2 provides a straightforward summary of military laser ocular hazards and protection, summarizing current knowledge for the soldier.

With the small, but increasing number of laser eye injuries associated with military target acquisition systems, the issue of suprathreshold laser-induced injury became increasingly important.³ These cases

revealed that laser-induced retinal damage need not be restricted to the central retina to have significant consequences for visual function. These consequences involve the development of intraretinal scar formation (IRSF), retinal traction generally associated with IRSF, and retinal nerve fiber layer (RNFL) damage. These secondary sequelae extend concern well beyond the macular region and, therefore, require new ophthalmic and functional techniques to assess development, progression, and the long-term consequences to visual function to distinguish normal functioning retina from dysfunctional retina. These new techniques must cover the full spectrum of visual function to include measures of contrast required to resolve features that subtend a range of visual angles, the ability to detect fine differences in hue, and sensory / motor coordination of fixation eye movements. The ability to diagnose deficits in such visual qualities currently limits the

EXHIBIT 5-1

THE ARMY MEDICAL DEPARTMENT'S ROLE IN DEVELOPMENT, DEPLOYMENT, AND USE OF LASERS BY THE MILITARY

Shortly after the invention of the laser in 1960, the military began to develop ways to utilize the new technology to assist in its many complex missions. Science fiction and the popular press speculated on the laser's potential and highlighted its use as a "ray gun" that could effectively engage both materiel and people rapidly (at the velocity of light) and with a "magazine" only limited by the power source. The laser was depicted as destructive to materiel at large distances, far exceeding those reached by most conventional munitions, albeit it did require line of sight. Concomitant with the desire to build high energy lasers to engage materiel was the development of low-power devices that could assist in the military's fire control and training missions. The laser's attributes included (a) monochromatic emission (one wavelength or color or emissions at multiple discreet wavelengths throughout the visible and infrared spectrums), (b) intense energy in a well-collimated beam (ie, a beam that does not spread much with distance), (c) emissions in extremely short duration pulses (ie, nanosecond exposure durations required for range finders), and (d) repetitive pulse or pulse-coded emissions. Laser range finders, laser target designators, and laser "live fire" training devices were under development to exploit the attributes offered by this emerging technology.

The potential for laser energy to injure the eye was recognized early, and research groups who had studied the ocular hazards of nuclear fireballs shifted their attention to laser radiation. Technology programs began within the Department of Defense (DoD) to exploit the characteristics of the laser for military applications from training and fire control to weapons systems. Potential adversaries also had laser expertise. The technology was scientifically robust and emerging worldwide with new wavelengths, high emission energies, shorter duration pulses, and applications that continue to exploit these advances.

Within a short period of time, a controversy arose surrounding the establishment of permissible exposure limits for the Q-switched ruby laser. The Army was developing the first ruby laser range finder at the Frankford Arsenal in Philadelphia, Pennsylvania. The Army Medical Department (AMEDD) recognized responsibility to ensure the health and safety of soldiers operating laser systems and understood that laser weapons would emerge on the modern battlefield and injure soldiers entrusted to care. Hence, the AMEDD established a joint research team at the Frankford Arsenal that combined the medical expertise of the AMEDD with the electronic, optics, optical fabrication, laser, and fire control systems expertise of the US Army Materiel Command. In 1968, the Joint US Army Materiel Command and the US Army Medical Research and Development Command Laser Safety Team (or the J AMC-AMRDC LST or simply the JLST) was established. The controversy on Q-switched ruby lasers was ultimately resolved, but many other laser issues continued to emerge.

Argon lasers had already made their way to the ophthalmology clinic, but other lasers were relatively new or rare and could not be purchased commercially. To support the biomedical research, optical delivery systems were interfaced to fundus cameras, and laser systems were fabricated on site at the Frankford Arsenal. The group generated data from which exposure limits could be derived; both ocular and cutaneous injury thresholds were determined as a function of laser wavelength, exposure duration, irradiance diameter, and pulse repetition frequency. Biological effects of ruby, neodymium, argon, carbon dioxide, erbium, and gallium arsenide diode lasers were investigated and reported.

In 1974 with the pending closure of the Frankford Arsenal, the AMEDD members of the JLST moved to the Letterman Army Institute of Research at the Presidio of San Francisco, California (Exhibit Figure E1-1). The research conducted in the 18 years at the Letterman Army Institute of Research (LAIR; 1974–1992) focused on medical issues surrounding the Army's use of lasers in a wide range of systems. High-energy laser systems were developed by the DoD to engage targets at large ranges. Low-energy lasers were used in many fire control and mission assist applications. Laser weapons were prominent in the DoD threat statements. Medical applications of lasers emerged, and by the early 1990s, laser use in hospitals was quite common in most medical specialties. Ophthalmological applications emerged very rapidly. Industrial hygiene and occupational health guidance was established and continually updated to facilitate the safe use of lasers in the workplace. This guidance was based on the maximum permissible exposures or exposure limits for optical radiation that were predominately supported by the triservice DoD research. In 1979, LAIR organized the first Lasers on the Modern Battlefield (LMB) Conference. The LMB quickly became the annual forum for issues surrounding the development, deployment, and use of lasers by the military, and provides a classified forum for interaction across programs and corps, including international partners.

(Exhibit 5-1 continues)

Exhibit 5-1 continued



Fig. E1-1. Key Laser Bioeffects Researchers at Letterman Army Institute of Research (LAIR), San Francisco, California. Pictured (left to right) are David Randolph, Bruce Stuck, Harry Zwick, Jack Lund, and Edwin Beatrice.

A 1980 symposium on Combat Ocular Problems became the watershed event that resulted in the first development of military protective eyewear. The focus of the conference was broader than the laser threat issue and included eye trauma. Colonel Francis LaPiana, an accomplished ocular plastic surgeon, postulated that more than 90% of the injuries from fragments in and around the eye that he had managed in the Vietnam War could have been prevented by a 3–4 mm thickness of polycarbonate (Lexan, a product of the General Electric Company, Fairfield, Conn). Lieutenant Colonel (Dr) Belkin, based on his experience as an ophthalmologist in the Israeli Defense Forces Medical Corps during the Six Day War in 1967 and the Yom Kippur War in 1973, made a similar argument. The human factor issues and limitations of protective solutions (absorptive dyes in glass or plastic) for laser protection were also discussed. The high attenuation of selected visible wavelengths for laser protection limited the overall visible light (luminous) transmission and distorted perception of the color space (inability to readily detect red warning lights with eye protection designed for ruby laser emissions at 694.3 nm). Although polycarbonate provided protection against fragments, there was no specification for fragment protection. Absorbing dyes introduced into the polycarbonate or surface preparations degraded the fragment protection properties, and polycarbonate was “soft” and difficult to edge if formed into corrective lenses. Polycarbonate was also very susceptible to scratches, and the lifetime of a spectacle or an aviator visor was estimated to be very short in a dusty/dirty combat environment. Although technology programs began to develop laser protection, there was no program addressing fragment protection.

(Exhibit 5-1 continues)

Exhibit 5-1 *continued*

Colonel Beatrice (Exhibit Figure E1-2), supported by his Commanding General, MG Rapmund, identified a clear Army need that was focused on protecting the soldier in development of laser and fragment protective eyewear. The team had a full research portfolio already, no budget for an eye protection program, and no official Army requirement, much less a complete picture of the acquisition process for materiel development. The soldier needed eye protection that he could function with day or night that protected against a few select laser wavelengths and ballistic fragments. Nevertheless, over the next 4–6 years, the Ballistic and Laser Protective Spectacles (BLPS) were developed. The laser protective clip-on was less than ideal, provided protection only against two common wavelengths used by the military, and had difficulties meeting the solarization specification. Saturation of absorbing dyes limited the protection against intense nanosecond pulses of laser radiation. The group developed saturation measurement methods, which have been adopted by the American National Standards Institute guidance for commercial laser protective eyewear. The BLPS program also produced visors for the HGU-56/P helmet (Gentex Corporation, Simpson, Pa) through active collaboration with the Army aviation materiel developer. Subsequently, the BLPS system was type classified, and some units in the first Gulf War were equipped. Although the BLPS system was the first fielded fragment and laser protective eyewear for soldiers, it never achieved overwhelming acceptance. However, the development and fielding process formed the basis for subsequent protective eye armor. Technical specifications developed for the BLPS program guide advancements in military protective eyewear development today. The Emerging Laser Threat Eye Protection (ELTEP) program was cancelled in 1991, with an understanding that protection outside the body (“skin out”) would be the mission of the PM (Project Manager) soldier, and the AMEDD would be responsible only for corrective lenses.



Fig. E1-2. Colonel Edwin S. Beatrice, leader of the Laser Bioeffects Research Team and later, Commander, Letterman Army Institute of Research (LAIR).

Laser bioeffects research at LAIR was as diverse as the developmental laser systems and their applications (both military and civilian). The Multiple Integrated Laser Engagement Simulator (MILES) was a class of gallium arsenide laser-based systems designed to simulate live fire during training with conventional weapons. The M-16 rifle version of the MILES device had soldiers directing lasers at other soldiers in training for the first time. The AMEDD, as well as the developer, wanted to ensure that the system was safe prior to widespread use. The team conducted a series of biological effects studies that expanded the understanding of laser bioeffects through investigations of the additive effects of repetitive pulses, the dependence of the retinal injury threshold on retinal irradiance diameter, and an understanding of the retinal effects of near-infrared laser radiation.

In October 1980, a Los Angeles Police Department helicopter was illuminated by an air-cooled argon ion laser that a technician had taken home to project Lissajous patterns on the wall for a Halloween party. Illumination of the Los Angeles Police Department helicopter crew resulted in evaluation of the pilot’s and co-pilot’s eyes and vision at LAIR, and an assessment of laser and exposure conditions. The laser obtained for inspection was operating at a wavelength of 448 nm; however, there was no retinal injury as would be anticipated by an overexposure at that wavelength. There was a corneal abrasion apparently due to rubbing the eye secondary to the startle when the bright intrabeam viewing experience occurred. The night illumination surprised the crew, and when they momentarily lost their visual cues, they were concerned about their safety and ability to safely fly the aircraft. Evaluation of the emission characteristics of the laser and the distance from the helicopter indicated that the exposure was well below levels required to produce retinal injury, but the laser glare at levels below the permissible exposure limit appeared extremely bright and compromised the crew’s ability to fly the aircraft. Suddenly, it was clear that laser glare, particularly under low luminance conditions (dawn, dusk, or night), could interfere with military operations and pose secondary hazards to soldiers or result in a

(Exhibit 5-1 continues)

Exhibit 5-1 continued

“soft” mission defeat. Consequently, laser glare studies in a terrain board pursuit tracking simulator built at the LAIR were initiated.

Emphasis was on threshold effects and research addressing the issue of potential long-term effects from laser exposure. Assessment of laser injury through enhanced ophthalmic imaging diagnostics (confocal scanning laser ophthalmoscopy, optical coherence tomography), novel visual function assessments, and emerging molecular biological assays complemented light and electron microscopy characterizations of laser-induced eye injury. The Aidman Vision Screener (AVS)—a 5 x 7 inch card with an acuity chart, Amsler grid, and evacuation criteria—was proposed to assist the combat medic in rapidly assessing laser-induced injury in an operational environment (Exhibit Figure E1-3). The AVS was accepted as a rapid screening tool and was type classified, and a new *US Army Field Manual 8-50* titled “Prevention and Medical Management of Laser Injuries” was drafted. *US Army Field Manual 8-50* was published in 1990 just before the first Gulf War.

In September 1992, the Division of Ocular Hazards moved to Brooks City-Base, San Antonio, Texas, to be collocated with the Air Force Research Laboratory’s Directed Energy Bioeffects Research and the Navy’s nonionizing radiation programs that were being relocated from Pensacola, Florida. Fifty Rhesus monkeys were also moved from the Presidio of San Francisco to Brooks Air Force Base. The US Army Medical Research Detachment–Walter Reed

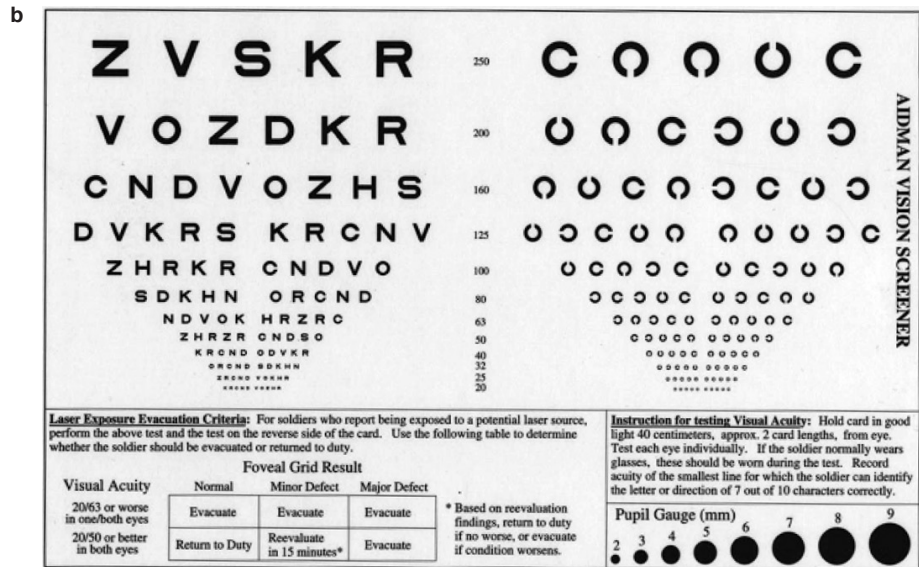
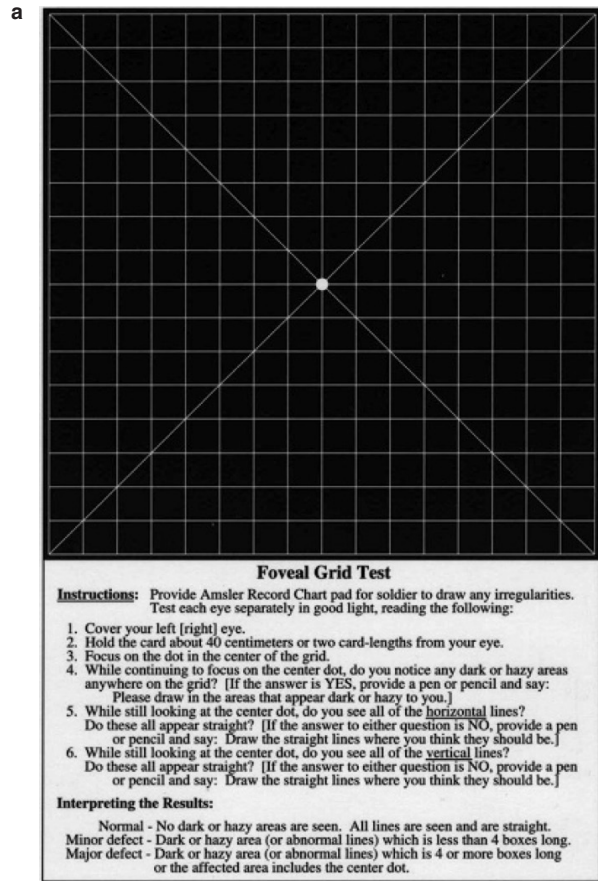


Fig. E1-3. The Aidman Vision Screener (AVS) assists the combat medic in rapidly assessing laser-induced injury in an operational environment. It provides an Amsler grid (a), a visual acuity chart, and evacuation criteria (b). The AVS is required to triage laser-induced eye injury in accordance with the guidance given in *US Army Field Manual 8-50*, “Prevention and Medical Management of Laser Injuries.” Washington, DC: Headquarters, Department of the Army; August 8, 1990. Photographs: Courtesy of the US Army Medical Research Detachment.

(Exhibit 5-1 continues)

Exhibit 5-1 *continued*

Army Institute of Research (USAMRD–WRAIR) executed its mission at Brooks Air Force Base from 1992 through 2010. The program continued to focus on acute laser bioeffects, addressing gaps in the biological database required to define optical radiation exposure limits pertinent to emerging military exposure conditions. These gaps were driven by military system developments, such as the emergence of the use of the oxygen iodine laser with emissions at 1.315 μm , the emergence of the use of “particle cells switches” against pulse lasers operating the retinal hazard spectral region, and a relook at laser glare issues surrounding the use of green laser illuminators to deter unknown encroachers on valued assets. The team provided vital technical advice and expertise to the Department of State in discussions of the “Blinding Laser Weapon Protocol” negotiated in Vienna, Austria, in 1995. Accidental laser eye injuries continued to occur within the military, and the unit assisted in their assessment through the use of advanced imaging (scanning laser ophthalmoscopy and optical coherence tomography) and measurements of visual function. The Laser Accident and Incident Registry was developed to archive these and other laser exposure injuries and incidents. Although laser-induced eye injuries were infrequent and predominately involved the misuse of lasers in military settings, the information obtained from these and other laser-induced eye injuries that occurred in the private sector were important to enhance the understanding of cases and the collection of cases that occur in industry, medicine, and research laboratories. (This is the focus of Chapter 5.)

Evaluation of corneal, lens, iris, and retinal injury threshold for laser wavelengths in the 1.1–1.4 μm region was driven by the DoD efforts to build high-energy lasers operating at the chemical oxygen-iodine laser (COIL) wavelength of 1.315 μm . Colocation of directed energy bioeffects research program at Brooks Air Force Base allowed collaboration and design of complementary research on these issues. A complex series of experiments addressed both the wavelength dependence and locus of ocular injury for exposures in the near infrared and dependence of the retinal injury threshold on retinal irradiance diameter. These studies resulted in major changes to optical radiation exposure guidelines.

High-powered laser diodes resulted in the proliferation of laser pointers, first red and now green, and the availability of high-power laser illuminators drew attention to laser glare and purposeful exposure issues. The team continued both laboratory and field studies of laser glare to assess the operation impact of noninjuring exposures. Investigations of natural protective mechanisms were conducted. The kinetics of the pupillary response and the aversion response (consisting of head or eye movement, squint, and blink), and a description of laser-induced after-images from the visible laser below the exposure limits were described. Eye movements were measured during deliberate fixations to more accurately assess the hazards of purposeful exposures. Data were used to develop the first retinal thermal injury model, wherein the source moved on the retina commensurate with the measured eye movements during deliberate fixation. With the emergence of wave front-corrected retinal imaging systems and to investigate the “worst” case viewing conditions, a series of experiments was conducted measuring the retinal injury threshold with the wave front correction for the optical aberrations in the eye that were exposed. This research, over a period of several years, was now critical to the adjustment of exposure limits for optical radiation.

Treatment of laser-induced retinal injury was addressed with a comprehensive study of the efficacy of steroids and nonsteroidal antiinflammatory agents on thermal lesions and pulsed lesions. Treatment studies were conducted to investigate regimens that could be initiated by first responders, followed by therapies administered later at higher medical care echelons. Applications of photodynamic therapy in the treatment of laser-induced eye injury were examined, as well as the use of optical radiation in the treatment of laser-induced retinal injury. Multifocal electroretinogram was applied to the assessment of focal, laser-induced retinal injury. Most recently, a series of studies has investigated applications of stem cells in the treatment of retinal trauma. Final treatment approaches will ultimately be based on the taxonomy of the lesion or injury. This work, along with the diagnostic imaging and novel assessments of visual function, stands as the basis for future ocular trauma.

ability to evaluate functional consequences of laser retinal injuries, particularly in differentiating between sequelae that is primarily retinal in origin from higher order sequelae.

This chapter presents the clinical evaluation of five military laser accident cases representing a range of laser-induced retinal damage. The assessment of each case will highlight the complexity of the structure–function relationship, as well as the importance of com-

binning imaging techniques to more precisely identify structural damage with the application of well-targeted functional assessments. The evidence presented herein demonstrates that functional diagnostic tools cannot be limited to neural mechanisms at the retina. As the structural damage resolves, processing of visual neural code along the visual pathway often produces visual function outcomes not immediately evident from the structural damage at the retina.

EXHIBIT 5-2

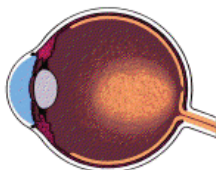
SUMMARY OF MILITARY LASER OCULAR HAZARDS AND PROTECTION



25-013-0498

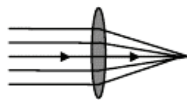
Just the Facts... Lasers and Their Effects on the Human Eye

➤ Eye Biology



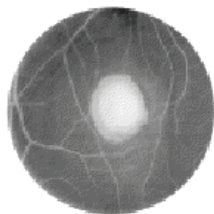
The Eye

➤ 1 to 100,000 Magnification



Property of the Eye

➤ Laser Damage



Laser Damage to the Retina of the Eye

Purpose.

To provide information and facts on the anatomy of the eye as it relates to laser eye exposure and the potential for laser eye injury.

Laser Effects on Visual Performance.

Figure 1 shows a soldier being exposed to a laser beam. Lasers may interfere with vision either temporarily or permanently in one or both eyes. At low-power levels, lasers may produce a temporary reduction in visual performance in critical military tasks, such as aiming weapons, driving a vehicle, or flying an aircraft. At high-power levels, greatly exceeding exposure limits, they may produce serious long-term visual loss or permanent blindness.

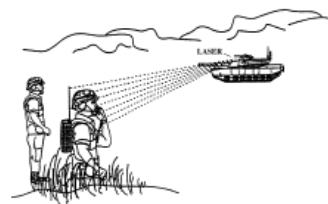


Figure 1

Anatomy of the Eye.

Figure 2 is a simple schematic of the eye. The following parts of the eye are important with regard to laser effects:

- The **Cornea**, a transparent front part of the eye, transmits most laser wavelengths except for far-ultraviolet and far-infrared radiation.
- The **Iris**, a pigmented diaphragm with an aperture (pupil) in its center, controls the amount of light entering the eye. During low-light conditions, such as in a dark room, visible and near-infrared lasers are slightly more dangerous since the pupil is larger than it would be in high-illumination conditions, such as in daylight.
- The **Lens**, a transparent structure located behind the pupil, which focuses light on the retina, allows visible and near-infrared energy to pass through while absorbing near-ultraviolet radiation.

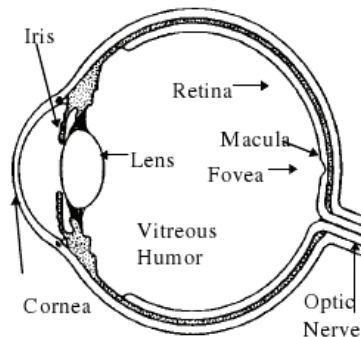


Figure 2

Laser/Optical Radiation Program
 U.S. Army Center for Health Promotion and Preventive Medicine
 ATTN: MCHB-TS-OLO, 5158 Blackhawk Road
 Aberdeen Proving Ground, MD 21010-5403
 DSN 584-3932 or Commercial (410) 671-3932

EMAIL: laser@amedd.army.mil INTERNET: <http://chppm-www.apgea.army.mil/laser/laser.html>

Reproduced from: the Laser/Optical Radiation Program, US Army Center for Health Promotion and Preventive Medicine (USA-CHPPM). Aberdeen Proving Ground, Md: USACHPPM. Technical Bulletin 25-013-0498.

The chapter begins with a discussion of imaging and visual techniques to assess retinal structure and visual function. This is followed by a brief discussion

of the integration of these techniques to determine structure–function relationships used to assess visual function in each of the five presented cases.

ASSESSING IN VIVO RETINAL MORPHOLOGY

Confocal Scanning Laser Ophthalmoscopy

Confocal scanning laser ophthalmoscopy (CSLO)⁴ provides the capability for imaging the retina along its axial dimension, yielding image “slices” in eyes with relatively large focal lengths, from the anterior RNFL-dominated retinal surface posterior to the retinal vasculature.^{5–7} Figure 5-1 shows CSLO images for a nonhuman primate (NHP; Figure 5-1a) and a garter snake (Figure 5-1c). NHP eyes have relatively large focal lengths, and the graph reflects the current state of the art in axial domain resolution (18 μm) for eyes with relatively large focal lengths. The art of the possible axial resolution is demonstrated in the garter snake eye, whose focal length is relatively short. For the NHP, however, the range of confocal slices is greater than for the snake eye. The optical properties of the NHP eye permit an axial range from the RNFL (Figure 5-1a) to the retinal vasculature (Figure 5-1b). The optical properties of the garter snake eye permit,

by comparison, a narrower range of axial separation, which is from the RNFL to the photoreceptor layer. However, the optical properties of the snake eye yield finer resolution of retinal structures than those of the NHP eye. This comparative CSLO work, imaging eyes of species with differing optical properties, reveals the advantage of imaging retinal elements and blood flow in the small eye. The small eye model allows for assessing damage to relatively fine retinal structure and for observing the repair cascade over time. New wave-front correction techniques utilizing adaptive optic algorithms to correct for optical aberrations of the imaged eye allow for diffraction-limited imaging in the “large” human eye. Confocal applications now allow observation of the photoreceptor and retinal pigmented epithelium (RPE) matrix in a human eye. These advances promise the detailing of morphological sequelae in the retina from the RNFL to the retinal vasculature to better understand and predict functional loss.

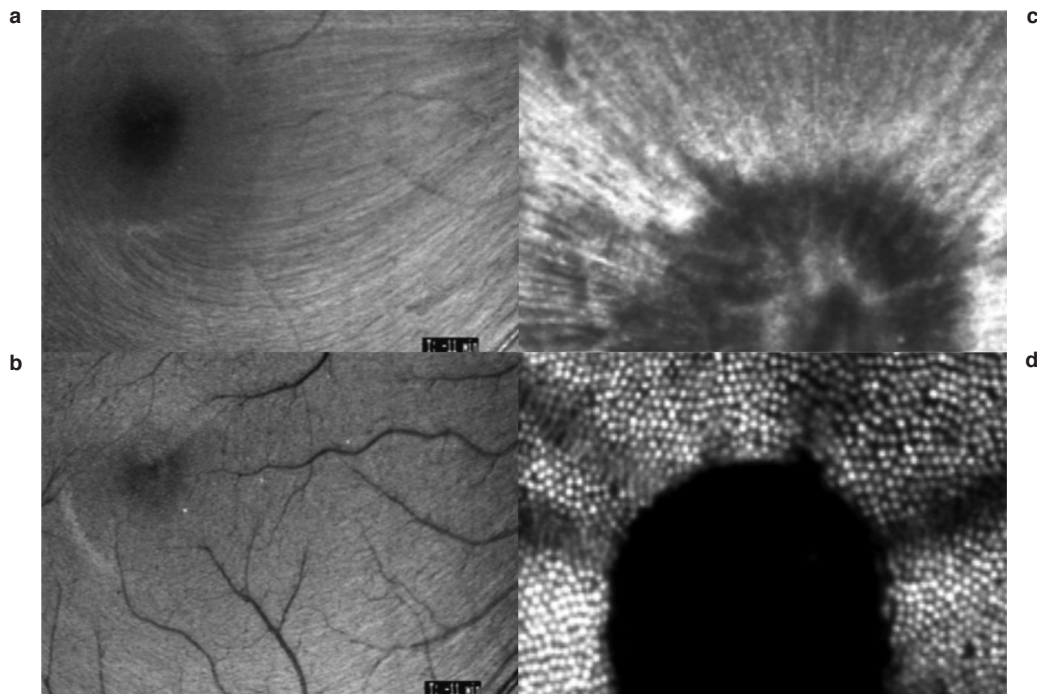


Fig. 5-1. Comparison of range of confocal slice between the Rhesus monkey (a, b) and the garter snake (c, d). Photographs: Courtesy of the Laser Laboratory, with the technical assistance of André Akers.

Optical Coherence Tomography

Optical coherence tomography (OCT) images provide an *in vivo* cross-section of the retina. Images are rendered in false color to indicate retinal layers and respective structures. Figure 5-2a shows the path of the OCT scan that rendered the image shown in Figure 5-2b. The figure shows the OCT-

rendered image taken through the macular region from the superior parafoveal retina into the foveal retina and ending in the inferior parafoveal retina. The thickness of the parafoveal retina is 250 μm and that of the foveal retina is 150 μm . These thicknesses correspond with histological retinal measurements and thus can be used to characterize the condition of the retina.

FUNCTIONAL METRICS AND STRUCTURAL CORRELATES

Assessing Visual Function Along the Visual Pathway

High spatial resolution vision (ie, visual acuity) is mediated by the central foveal region.⁸ Visual acuity demands a higher order neural integration and augmentation, thus resulting in a relatively robust visual function. It is, therefore, not surprising that foveal retinal damage must be extensive, with a significant degree of secondary damage, to result in a significant loss in visual acuity. Maximal visual spatial resolution, measured as visual acuity, is mediated at the center of the fovea. There, ganglion cells were originally thought to innervate the most central region of foveal photoreceptors in a ratio of 1 ganglion

cell to 1 photoreceptor,⁹ resulting in an off-axis acuity function, with a characteristic peak at the fovea and sharp declines in acuity with distance from the foveal axis.¹⁰ However, more recent work by Curcio et al^{11,12} has demonstrated that the central foveal cones have a 2:1 ratio with retinal ganglion cells. When the 2:1 ratio is accounted for in the off-axis acuity function, a resulting small plateau of maximal acuity over the central foveal retinal space is revealed.¹² This structure–function relationship suggests that neural plasticity associated with central foveal cones may actually begin in the inner retina. At the inner retina, central foveal cone innervation with ganglion cells via Henle’s fibers proceed to striate cortical visual space where the foveola ($\approx 150 \mu\text{m}$) is represented in a magnification of 7:1. In healthy visual systems, acuity provides a general measure of visual function. In laser accident cases where damage is confined to local areas of the retina, visual acuity is often insensitive to associated visual function changes because there is significant neural plasticity/redundancy associated with visual acuity.

Contrast sensitivity, on the other hand, measures the reciprocal of the minimal contrast required (sensitivity) for detection of visual stimuli across spatial (size) or temporal (target flickered on/off) frequencies. Stimuli are modulated sinusoidally across light and dark bands subtending a specific visual angle in the spatial domain and across on/off cycles in the temporal domain. The spatial contrast function yields a relatively lower order assessment of retinal integrity (magnocellular/parvocellular ganglion cell systems) because higher order processing of spatial information tends not to compensate for anomalies at the retina.¹³ Furthermore, measurements of temporal contrast sensitivity indicate contrast sensitivity of the paramacular retina targeting the more transiently responding magnocellular system, which is involved in directing gaze to the more sustained responding, centrally dominated parvocellular system.¹⁴ Thus, the forms of the spatial and temporal contrast sensitivity functions provide a complete picture of threshold sensitivity across target size to

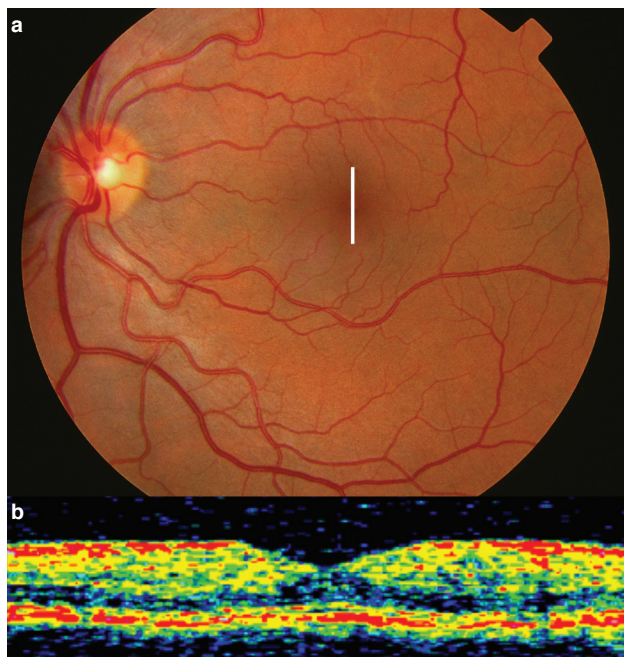


Fig. 5-2. (a) Vertical scan through the fovea. (b) OCT image yields a full retinal thickness cross-section of the scanned retina.

Photographs: Courtesy of the Laser Laboratory, with the technical assistance of André Akers.

register detection and movement predominately at the level of the retina.

As with visual acuity, traditional clinical color vision metrics, such as the Farnsworth Munsell 100 Hue (FM 100 Hue), are of limited utility due to their inability to accurately measure individual cone system damage. This is primarily because they involve measurements along the color (hue) discrimination dimension, which is not a direct measure of individual cone viability, but rather is a measure of the neural reorganization of cone input that takes place in the inner layers of the retina.

The FM 100 Hue presents hues along the entire cycle of the color wheel. Given that the colors and their discrimination scores represent a position in the cycle of hues, one can pattern the data using frequency domain time series models.¹⁵ Figure 5-3 shows the FM 100 Hue polar plots and their corresponding frequency density plots for a person whose vision is within normal limits (Figure 5-3a), a person with a congenital color deficiency (Figure 5-3b), and a laser accident case (Figure 5-3c).¹⁶ The resultant frequency density plots from a Fourier transform reveal the content of the color vision error function along the color circle, and quantify the relative contributions of the primary color deficit F1 and the primary deficit axis F2. F0 gives the average magnitude of error along the color circle. The remaining components are analogous to harmonics suggestive of the magnitude of sequelae. Relatively symmetrical axis deficits are typical of congenital defects (Figure 5-3b), with weak

F1 contributions suggestive of a primary color deficit. In laser cases (Figure 5-3c), significant F1 and F2 contributions exist. The F1 contribution is suggestive of the extent of the retinal ablation of cone type, and F2 is suggestive of disruption of higher opponent processes.

The FM 100 Hue presents a focal target of color and, as such, may be less sensitive to outer retinal photoreceptor assessment with regard to exposure effects that present with minimal ophthalmoscopic evidence of damage, but with subjective awareness of visual dysfunction. Under these conditions, several metrics involving outer retinal assessment have demonstrated the effectiveness of spectral sensitivity measures for visual acuity criteria. These permit measurements of spectral sensitivity functions that are made sensitive to parafoveal and foveal retina by manipulation of spatial resolution (acuity) criteria,^{17,18} as well as the development of color contrast grating techniques¹⁹ and the application of equal luminance color acuity charts.²⁰ The Rabin charts are especially notable in that they bring the capability to assess specific cone system functionality from the laboratory environment to that of the clinical environment. This capability is being applied to the current Aidman Vision Screener.²¹ The improvement to the screener uses spectral logMAR acuity targets with and without neural opponent chromatic backgrounds; this advancement promises the capability of diagnosing exposure effects that present with minimal ophthalmoscopic evidence.²²

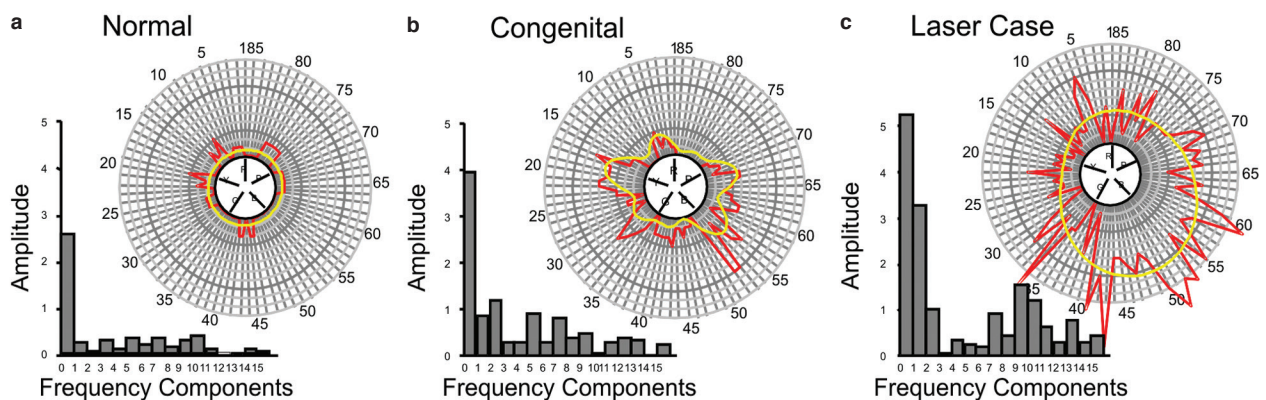


Fig. 5-3. FM 100 Hue test metrics for a human subject with normal color discrimination function (a), a human congenital color-deficient subject showing a bipolar deutan axis with a significant 2nd-order Fourier frequency component (b), and a human laser accident case (c) at 3 months postexposure showing a significant tritan monopolar error score and a highly significant 1st-order Fourier harmonic component. The axes of the FM 100 Hue test indicated in the center of the radial plots are as follows: B, blue; G, green; P, purple; R, red; and Y, yellow.

Illustrations: Courtesy of the Laser Laboratory, with the technical assistance of André Akers.

Integrating Imaging With Visual Function

Two separate techniques have been developed by US Army Medical Research Detachment-Walter Reed Army Institute of Research researchers to assess the functionality of laser-damaged retinal sites. In the first technique, the CSLO raster pattern is modulated to provide a sufficient range of Landolt ring gap sizes (Figure 5-4).²³ The technique is used to determine a contrast sensitivity function for local retinal areas. The operator can place the visual stimulus, via the CSLO raster, on areas of the retina that are of clinical interest and that generate contrast sensitivity functions for those areas. In this way, the operator can interrogate morphologically anomalous regions suspected of laser-induced damage. This technique is particularly effective when the ophthalmoscopic evidence is equivocal, even though there is a visual complaint associated with suspected exposure.

A second technique utilizes normal fixation eye movement pattern technology²⁴ to evaluate individuals with laser-induced retinal damage. Such patterns have been shown to produce minimal visitation in retinal regions that are dysfunctional, thereby providing a “map” of functional and nonfunctional retinas based on the frequency of ocular motor visitation (Figure 5-5). Figure 5c shows the typical normal foveal fixation pattern. This pattern takes the general form of an ellipse, with the larger axis along the temporal/nasal

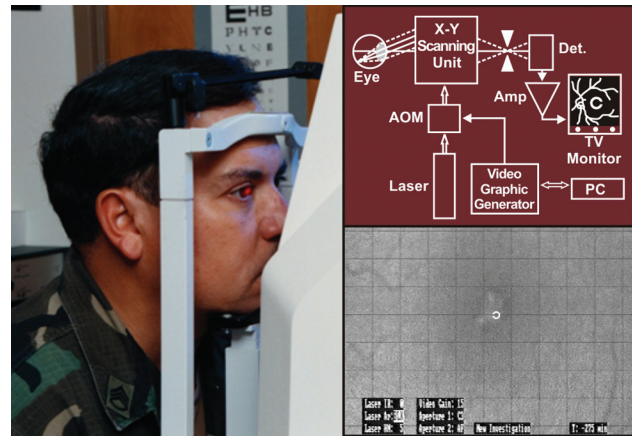


Fig. 5-4. CSLO imaging of visual function test target placement on a patient’s retina during measurement of contrast sensitivity. The schematic shows customized CSLO design, where Amp is amplifier, AOM is acoustic-optic modulator, Det is detector, PC is personal computer, and C is a Landolt C projected directly on the retina. Photographs/Illustration: Courtesy of the Laser Laboratory, with the technical assistance of André Akers.

extent typically spanning 150 μm . Deviations from this pattern are strongly associated with disruptions in the sensory matrix, which impact governing of the motor system directing eye movements.

LASER ACCIDENT CASES

The five military laser-retinal accident cases presented here were all associated with laser-induced macular retinal hemorrhage. All cases were evaluated using the techniques described previously. Four were induced by military laser range finders and one was

induced by a laser designator. Despite similarities in dose for the first four cases, lesion location is revealed to be critical to outcome, but in ways not predicted by central/peripheral convention. Case 5 is comparable with case 4 in lesion placement and highlights the

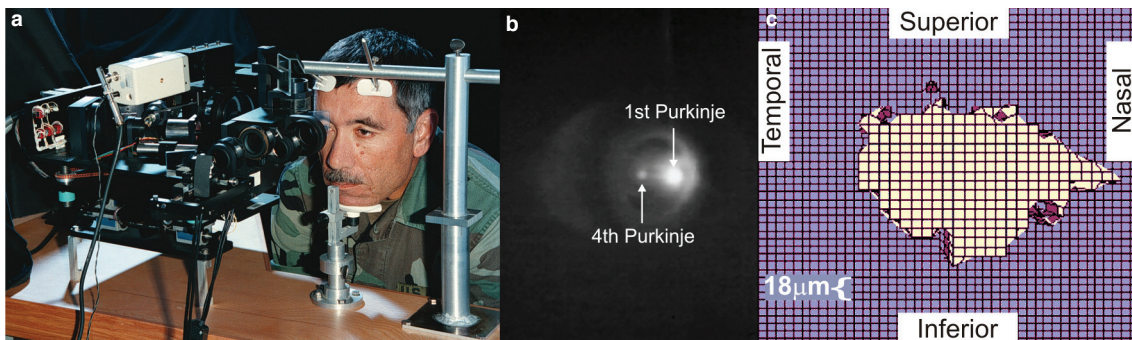


Fig. 5-5. A normal eye movement map (c) acquired using an SRI Dual Purkinje Eye-tracker (SRI International, Washington, DC) (a) from a patient who had reacquired normal fixation. (b) The 1st and 4th Purkinje images that are used to determine fixation to within 1 minute of arc and to differentiate eye rotation from head translation. Photographs/Illustration: Courtesy of the Laser Laboratory, with the technical assistance of André Akers.

importance of sensory and motor relationships, as well as the plasticity of the ocular sensory/motor system in reestablishing the visual system's ability to resolve fine-resolution targets.

Case 1

Case 1 received multiple accidental exposures to the right eye (OD [oculus dexter; pertains to the right eye]) from an AN/GVS-5 laser range finder with an operating wavelength of 1064 nm at an energy output at the aperture of 15 mJ/pulse. The range finder was held at arm's length from the eye and delivered several pulses with an estimated total intraocular energy (TIE) of 2.0 mJ per pulse, which resulted in 4 retinal lesions, 2 of which produced vitreous hemorrhages. (TIE is the total energy through the pupil that can be focused on the retina. If the total corneal radiant exposure is 10 mJ/cm² and the pupil diameter is 5 mm, then TIE = 10 mJ/cm² * 0.196 cm² = 1.96 mJ. Pupil diameter is estimated based on light conditions at the time of exposure.) These two hemorrhagic exposures occurred nasal and temporal to the macula, and a bridging scar though the foveal region was evident by 5 days postexposure.^{25,26} Figure 5-6 shows the resulting intraretinal scar at 18 months postexposure.

Measurement of visual acuity in OD at 24 hours postexposure was 20/400 and at 3 months postexposure improved to 20/200. Measurements of visual

acuity for this case, made over a subsequent 2-year postexposure period, remained unchanged at 20/200 (OD) and in the unexposed eye at 20/20 (OS [oculus sinister; pertains to the left eye]). Spatial and temporal contrast sensitivity functions measured at 6 months postexposure, using the CSLO technique described previously, showed both high- and low-spatial frequency deficits. Figure 5-7 shows the maximum difference in spatial (stationary) and temporal (dynamic) contrast sensitivity functions between OS and OD. The spatial contrast sensitivity function shows the largest difference at approximately 4 cycles/degree, with the peak of the normal function at 6 cycles/degree. Furthermore, suppression for targets >4 cycles/degree is greater than for targets <4 cycles/degree. This indicates that there is significant disruption to both magnocellular and parvocellular systems, with the magnocellular system disruption having a larger contribution to the overall visual function deficit.

The temporal contrast sensitivity function confirms the larger contribution of the magnocellular system disruption to the overall visual function deficit. The temporal contrast sensitivity function (Figure 5-7, dynamic) shows that, for sinusoidal targets, luminance modulated at 1 Hz and maximal deficit is at 1 cycle/degree. Under these measurement conditions, the typical temporal contrast sensitivity function peaks at 4 cycles/degree.²⁷ The fact that the largest deficit for spatial contrast was in the low- to mid-spatial frequency (4 cycles/degree) and that the temporal contrast

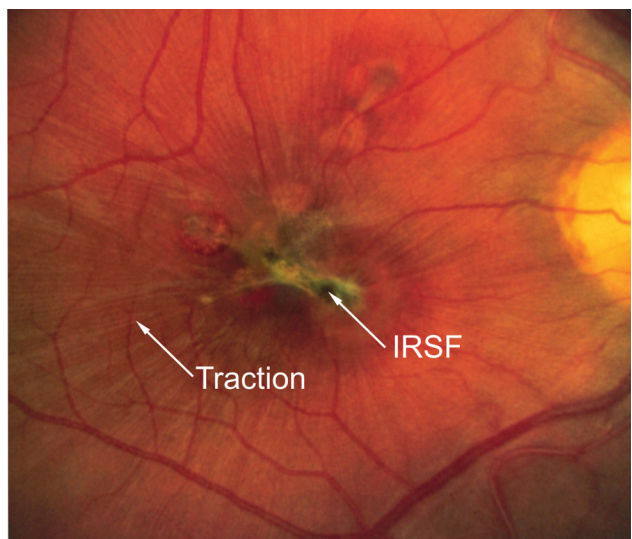


Fig. 5-6. Case 1: multiple exposures about the fovea and IRSF between two of these lesion sites. Retinal traction extending from the IRSF is evident well beyond the macula. Photograph: Courtesy of the Laser Laboratory, with the technical assistance of André Akers.

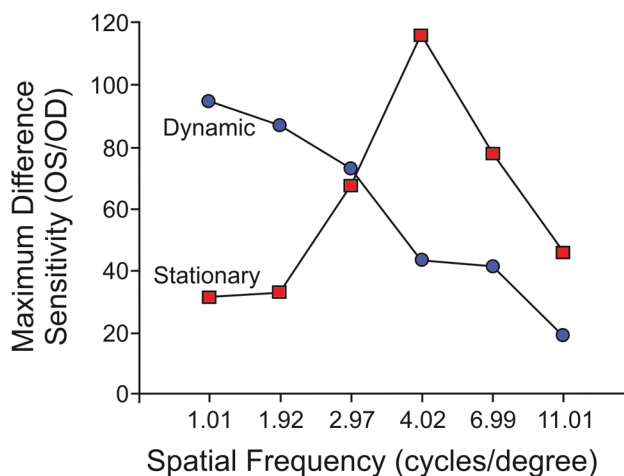


Fig. 5-7. Measurements of stationary and dynamic contrast sensitivity (1-Hz luminance modulation) reveal maximum deficits in contrast sensitivity at 4 cycles/degree stationary and 1 cycle/degree dynamic. Illustration: Courtesy of the Laser Laboratory, with the technical assistance of André Akers.

sensitivity peak is shifted to the higher spatial frequencies (deficit is smallest at 11 cycles/degree) further confirms magnocellular system disruption. Note in the fundus photograph (Figure 5-6) the extensive parafoveal traction, a secondary sequelae from the tension caused by the contracting intraretinal scar. The traction may be contributing to the magnocellular system deficit, since the magnocellular pathway arises principally from the parafovea.

Color deficits were assessed in the exposed eye (OD) with the FM 100 Hue test. Tests were performed 6 months subsequent to exposure and were given with and without fixation restrictions. Figure 5-8 shows the resolving of the color deficit from a large average relatively undifferentiated deficit weighted toward the blue to an average deficit within normal limits, but nonetheless showing anomalies in the blue, green, and purple. Of note are the distinct clusters of frequency components for the restricted fixation conditions measure. The frequency component distribution shows a very large overall deficit (f_0) and a strong unipolar component (f_1), which is a strong blue weighting. The cluster of frequency components beyond f_6 are indicative of the lack of a well-formed system to govern color discrimination, most likely a result of an inability to reliably fixate areas of the retina structurally intact enough to make a discrimination due to test-imposed fixation restrictions. When fixation restrictions were relaxed, the deficit resolved to a more well-formed frequency component distribution showing an overall deficit at f_0 , a weighting to the blue (f_1) with differentiated green and purple

contributing anomalies, and a nominal red pole (f_4). The persistence of the blue (S cone) anomaly across conditions is consistent with paramacular injury and magnocellular system disruption.²⁸ That is because medium and long wavelength-sensitive cones are concentrated almost exclusively in the fovea, whereas short wavelength-sensitive cones are principally distributed parafoveally, and signals from these cones are carried by the magnocellular pathway. Thus, parafoveal damage impacts the chromatic system principally by disrupting the perception of blue and related hues. The color discrimination results are confirmatory of the contrast sensitivity results, indicating a strong magnocellular system disruption. Furthermore, the fundus showed only paramacular lesions, with the insult to the fovea due to the intrusion of an intraretinal scar. Visual field analysis did show functional central retina in the vicinity of the scar, and, thus, when fixation restrictions for the FM 100 were relaxed, color discrimination improved to within normal limits, albeit with anomalies evident in the blue and related hues.

Case 2

Case 2 received bilateral accidental exposures from an AN/GVS-5 laser range finder with an operating Q-switched wavelength of 1,064 nm with an energy output at the aperture of 15 mJ/pulse. The range finder was held about 0.6 m from the eyes and delivered at least 2 pulses with an estimated TIE of 1.0 mJ per pulse, which resulted in bilateral retinal lesions

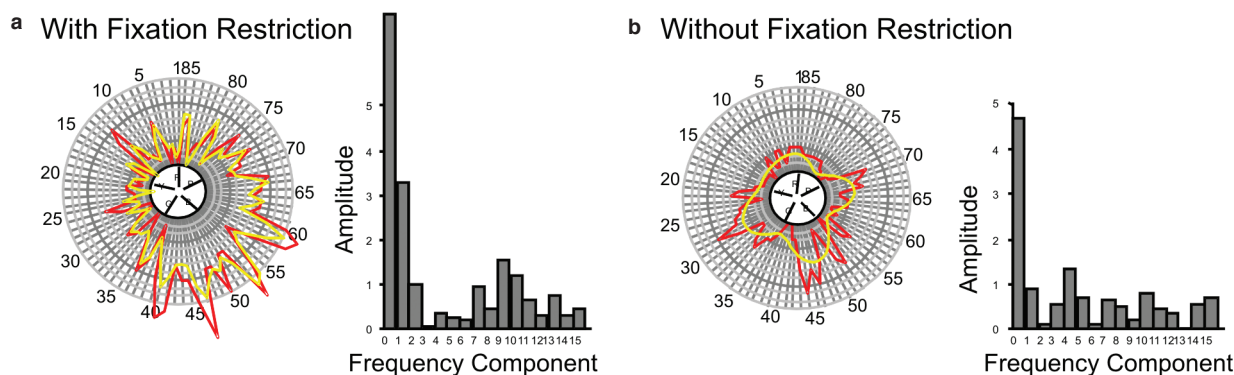


Fig. 5-8. FM 100 Hue scores for the affected eye (OD) show a shift (a) from a large fundamental indicating a large average error with a strong 1st harmonic that is indicated in the graph as a strong blue deficit that diminishes (b), when fixation restrictions are relaxed, to an average error within normal limits although with significant 1st and 4th harmonic components. The axes of the FM 100 Hue test indicated in the center of the radial plots are as follows: B, blue; G, green; P, purple; R, red; and Y, yellow.

Illustrations: Courtesy of the Laser Laboratory, with the technical assistance of André Akers.

that produced macular holes. The focus of this case is the sequela observed in the right eye (OD) over a 2-year period.

OD received a paramacular exposure temporal to the optic disk and nasal to the macula in the papillo-macular bundle (PMB). The lesion produced a vitreous hemorrhage in this region that required about 3 weeks of postexposure to resolve. The lesion itself eventually developed into a full-thickness paramacular hole. Immediately following exposure, visual acuity was 25/50 (OD); at 3 weeks postexposure, visual acuity was 20/70 (OD); and by 13 months postexposure, visual acuity deteriorated to 20/800 (OD) postsurgery. At 13 months, contrast sensitivity was not measurable beyond 6 cycles per degree.

Figure 5-9 shows the CSLO image of the paramacular hole, the CSLO image of the PMB-RNFL defect (Figure 5-9a), and an OCT scan through the center of the paramacular hole revealing complete loss of sensory retina (Figure 5-9b). The dotted outline shows the extent of RNFL pruning in the region of the PMB showing a wedge defect. This particular defect was first described by Frisch et al.²⁹ Zwick et al.³⁰ later modeled the phenomenon in NHPs to investigate the functional implications of the laser-induced retinal neural pruning that was shown to progress with Wallerian degeneration.

Figure 5-9c shows the fixation eye movement patterns at 18 months postsurgery, which removed epiretinal scar tissue that was producing traction

that was inducing retinal detachment. The map of functional retina rendered by this technique allows for the assessment of functional retina from which to interpret the images of structural damage. Normal fixation eye movements map in an elliptical pattern, with the majority of visitation times within the fovea. The average extent of the nasal/temporal axis of the elliptical pattern is $\approx 150 \mu\text{m}$ and that of the superior/inferior axis $\approx 100 \mu\text{m}$.³¹ Comparatively, the fixation eye movement pattern shown in Figure 5-9c suggests a lack of strong sensory input to govern the eye movements. Although there appears some visitation in the area of the fovea, there is also a significant amount of searching around the functional boundary of the macular hole. Together this suggests that the remaining sensory retina produces insufficient signal quality to govern target fixation. Note the irregular shape of the boundary of functional retina, and that the rendered map does not mirror exactly the size and shape of the hole. The functional map is dependent not only on the integrity of the neural elements, but also on the communication between sensory and motor systems. Thus, disruption in pathways will affect the functional map such that areas not visited in the eye movement map may appear relatively well formed in the structural imagery. The Wallerian degeneration of nerve fiber in the PMB can account for the differences between structural and functional imagery. Nonetheless, without the structural image showing nerve fiber track pruning, the functional map cannot be differentially interpreted.

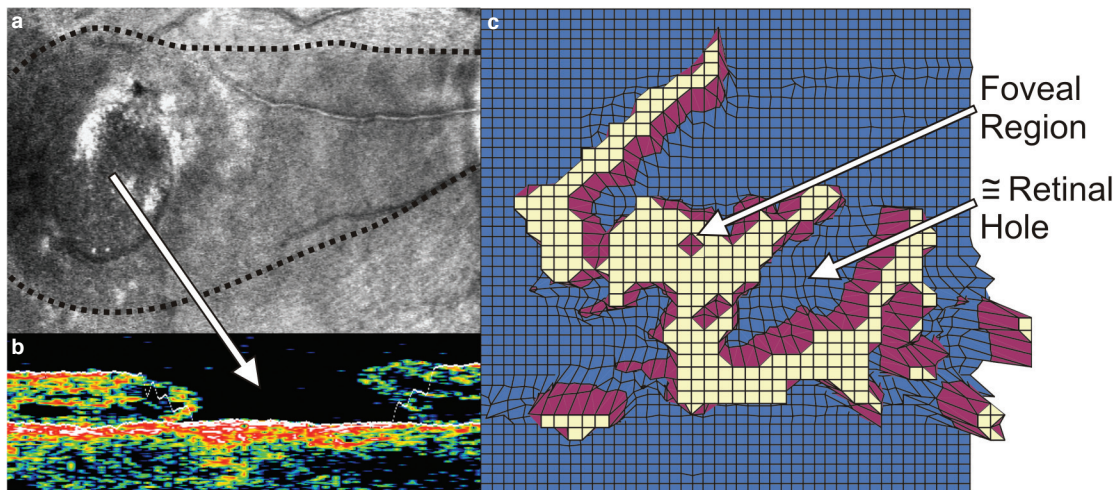


Fig. 5-9. (a) CSLO image of OD paramacular hole taken after stabilization surgery at 18 months postexposure. **Dashed outline** shows the RNFL defect. (b) OCT scan through this hole (**arrow**) showing loss of sensory retina leaving retinal pigmented epithelium and choroidal vasculature. (c) Fixation eye movement map obtained for OD postsurgery. Map shows a dysfunctional fixation pattern, with fixation at any one location minimal. The grid is $\approx 400 \times 400 \mu\text{m}$; 1 grid square is $\approx 9 \mu\text{m}$. Photographs/Illustration: Courtesy of the Laser Laboratory, with the technical assistance of André Akers.

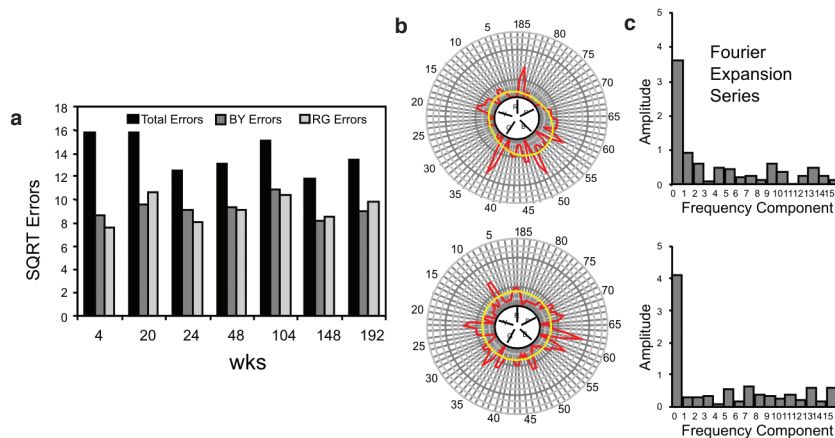


Fig. 5-10. (a) FM 100 Hue scores show no trends in total error scores. The frequency composition shows a transition in the distribution from (b) first harmonic contribution suggestive of a monopolar blue weighted deficit at 4 weeks postexposure to (c) a large f0 undifferentiated error at 192 weeks, suggesting an inability to discriminate color. The axes of the FM 100 Hue test indicated in the center of the radial plots are as follows: B, blue; G, green; P, purple; R, red; and Y, yellow. BY: blue-yellow; RG: red-green; Sqrt: square root error; wks: weeks
Illustrations: Courtesy of the Laser Laboratory, with the technical assistance of André Akers.

Figure 5-10 shows FM 100 Hue color discrimination error scores over 192 days postexposure. There appears to be no trend in total and partial error scores, with all scores well beyond normal limits. The long-term absence of any significant harmonic frequency component indicates that the trichromatic receptor

components have been equally affected (Figure 5-10c). This is most likely caused by the Wallerian neuronal degeneration observed in the PMB. These fibers transmit trichromatic cone output from the 3rd-order neuron to higher brain regions that require this input for color discrimination.

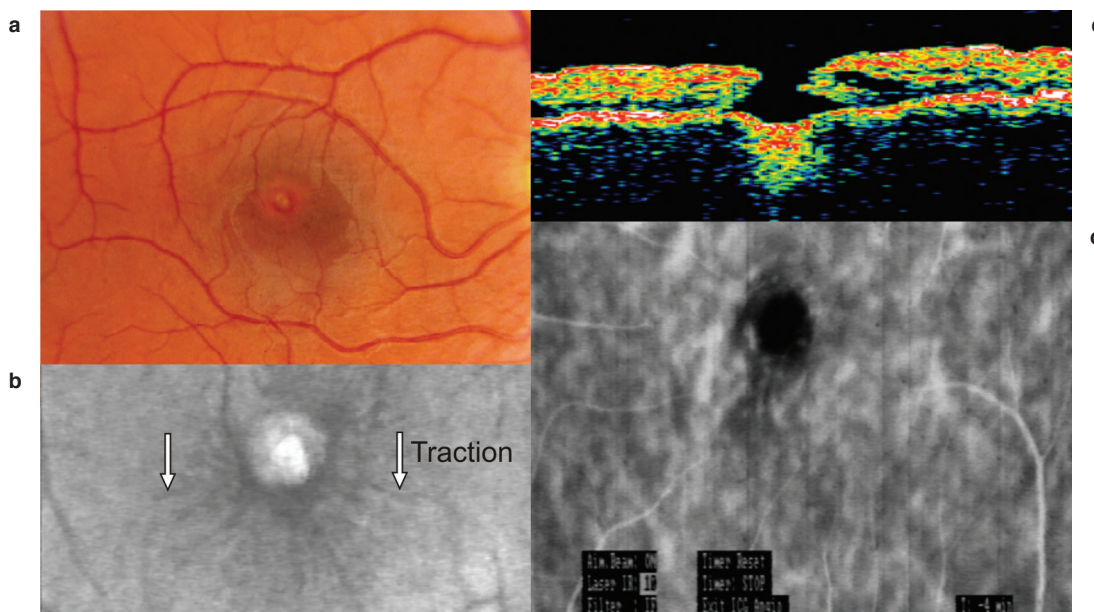


Fig. 5-11. A full-thickness fundus photograph of the macular hole at 3 months postexposure (a), corresponding CSLO image showing evidence of traction (b), OCT vertical scan through the center of the macular hole (c), and a CSLO indocyanine green image with reflections indicating macula choroidal vasculature blockage (d).
Photographs: Courtesy of the Laser Laboratory, with the technical assistance of André Akers.

Case 3

Case 3 received unilateral (OD) accidental exposure to a 1,064 nm beam emitted by a battery-operated Nd:YAG laser range finder. The exit port of the range finder was held approximately 0.6 m from the eye. The eye received an estimated TIE of 2.5–3.0 mJ per pulse, which produced vitreal hemorrhage.³² By 3 weeks postexposure, the vitreous hemorrhage had cleared. A full-thickness 100- μ m diameter macular hole with evidence of traction was diagnosed at the 3-month postexposure fundus examination (Figure 5-11a,b). An OCT image taken through the center of the lesion site (Figure 5-11c) revealed total loss of sensory retina in the macula hole and a significant choroidal extension beneath the fovea. Reflectance in the CSLO indocyanine green (a clinical imaging technique using dye to evaluate blood flow in the retina) image indicated vascular blockage (Figure 5-11d). At 12 months, CSLO images revealed a reduction in hole size, the disappearance of traction bands, and changes in the choroidal entity appeared weaker in reflectance but broader in extent (Figure 5-12a). OCT showed evidence of tissue bridging the gap of the macular hole consistent with spontaneous reduction of the macular hole size (Figure 5-12b).

Visual acuity changed concomitantly with evidence

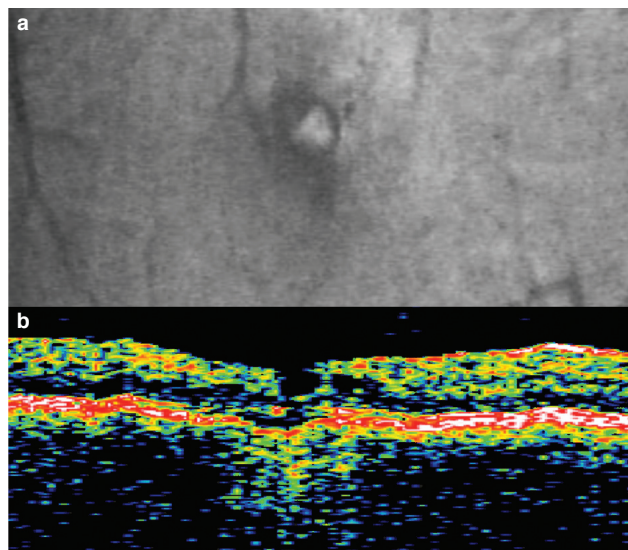


Fig. 5-12. Macula hole diameter is reduced in size at about 12 months postexposure compared with 3 months postexposure (see Fig. 5-11). (a) CSLO reveals an absence of retinal traction about the macular hole. Changes in choroidal entity appear weaker in reflectance at 12 months, but broader in extent. (b) OCT shows tissue bridging the gap of the macular hole. Photographs: Courtesy of the Laser Laboratory, with the technical assistance of André Akers.

of improvement in macular integrity. On presentation, visual acuity was 20/150 OD and 20/20 OS. At 3 weeks, visual acuity improved to 20/60 OD, declined to 20/70 at 3 months, and improved to 20/40 by 12 months postexposure. Color discrimination FM 100 Hue functions were within normal limits at 12 months, with no further change observed at 24 months postexposure. Contrast sensitivity measured using the CSLO technique showed a long-term deficit OD in sensitivity for high-spatial frequency targets (Figure 5-13).

Fixation eye movement patterns at 3 months were dominated by a vertical search pattern (Figure 5-14a). The vertical pattern spans an area greater than that of the foveal region. This pattern indicates a search for sensory retina to attract fixation eye movements. At 3 months postexposure, focal areas of functional sensory retina were unable to produce a strong enough signal to govern eye movements. At 12 months postexposure, the fixation eye movements showed an attraction focus and the development of a significant horizontal component. This component spans the typical $\approx 150 \mu$ m extent. However, the persistence of the vertical component suggests that the signal attracting eye movement visitations is weak (Figure 5-14b).

Case 4

Case 4 received bilateral accidental exposures from an AN/GVS-5 laser range finder with an operating Q-switched wavelength of 1,064 nm producing an

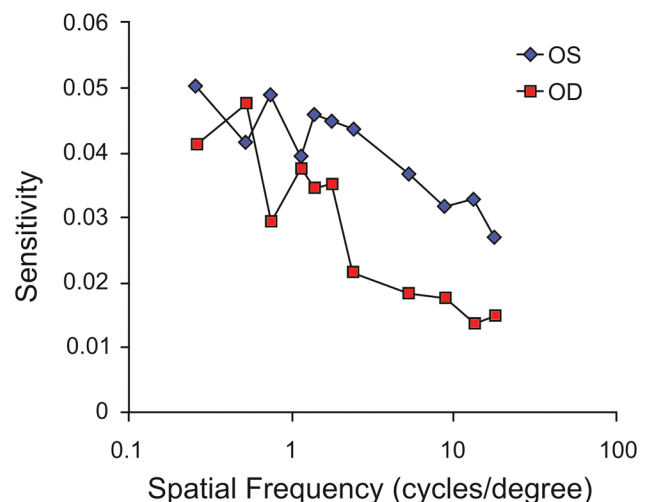


Fig. 5-13. Contrast sensitivity measured using the CSLO technique showed a long-term OD deficit in sensitivity for high-spatial frequency visual stimuli. Note the significant suppression in OD sensitivity from 6 to 30 cycles/degree. Illustration: Courtesy of the Laser Laboratory, with the technical assistance of André Akers.

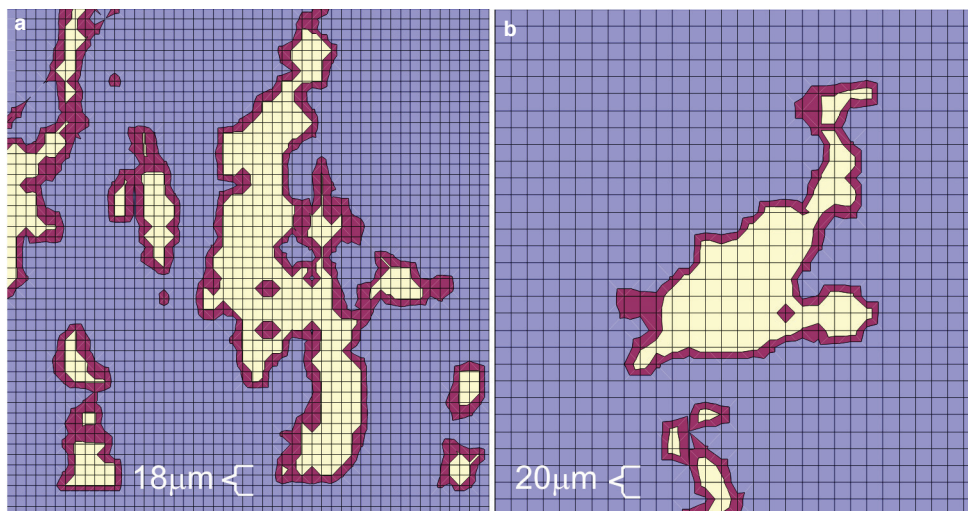


Fig. 5-14. Fixation eye movements changed significantly from 3 months (a) to 12 months (b) postexposure. At 3 months, an atypical vertical movement was observed that spanned over a 300- μm vertical range with little horizontal movement. At 12 months, fixation eye movements show a definite focus and a more typical horizontal extent (b). (Scale a: 1 box = 6 μm ; scale b: 1 box = 10 μm .)

Illustrations: Courtesy of the Laser Laboratory, with the technical assistance of André Akers.

energy output at the aperture of 15 mJ/pulse. The range finder was held about 0.6 m from the eyes and delivered at least 2 pulses, with an estimated TIE of 1.0 mJ per pulse, which resulted in bilateral retinal lesions that produced macular holes. The focus of this case is on the sequelae observed in the left eye (OS) over a 2-year period.

OS suffered an acute macular vitreous hemorrhage, with long-term damage restricted to the fovea. Figure 5-15 shows a fundus (Figure 5-15a) and CSLO image (Figure 5-15b) demonstrating a discontinuity through the center of the fovea. Figure 15c shows an OCT image revealing the extent of a small flat macular hole through the center of the fovea.

Visual acuity at 48 hours postexposure was 20/200; by 8 days postexposure, visual acuity improved to 20/25; and, by 3 years postexposure, visual acuity improved to 20/15. Color discrimination measured with the FM 100 Hue test at 3 years postexposure demonstrated error scores within normal limits, with no significant axis or harmonic components.

Landolt ring contrast sensitivity measured under CSLO retinal observation confirmed that foveal placement was not used in distinguishing small Landolt ring targets normally requiring foveal utilization. Instead, such targets were consistently placed superior and slightly temporal to the fovea. The contrast sensitivity function peaked at the typical 6 cycles/degree, and sensitivity across spatial frequency was within normal limits, although at the lower limit (Figure 5-16).

At 4 years postinjury, visual acuity was recorded at

20/15. Figure 5-17 shows the fixation eye movement patterns at this time, the focus of which is consistent with that of the earlier CSLO observation (Figure

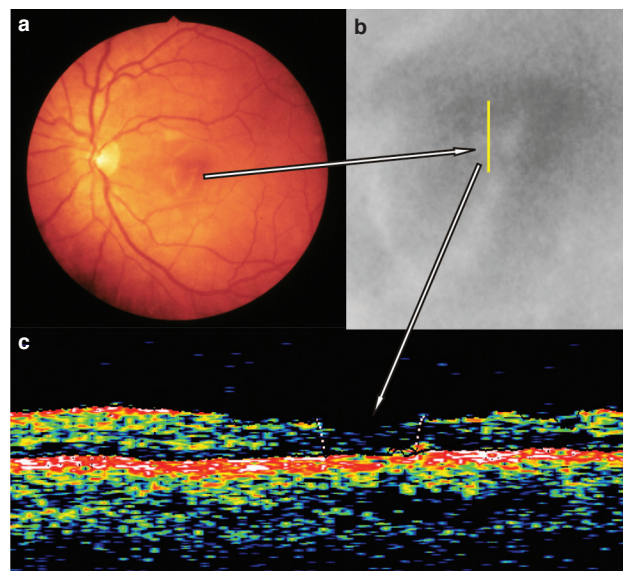


Fig. 5-15. The fundus photograph (a) shows a central anomaly in the macular area (**light spot** in center of the typical darker central macular area). The CSLO image shows a small foveal break in the retina and the track of the OCT scan across the break (b). The OCT image shows a small flat central hole (c).

Photographs: Courtesy of the Laser Laboratory, with the technical assistance of André Akers.

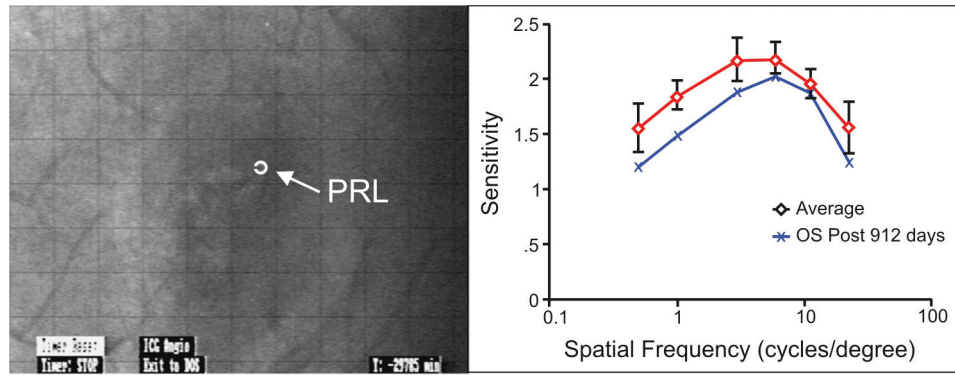


Fig. 5-16. The CSLO image shows contrast sensitivity test for the preferred retinal location for resolving fine-resolution targets (a). Placement of fine-resolution targets is superior and temporal to the fovea. Contrast sensitivity measured at 912 days postexposure shows a contrast sensitivity function within, although at the lower limit of normal (b). PRL: preferred retinal location

Photograph/Illustration: Courtesy of the Laser Laboratory, with the technical assistance of André Akers.

5-16a). The focus of the fixation eye movements tracks along the superior boundary of the foveal hole. The map of the eye movements about a focus superior and slightly temporal to the anatomical fovea shows a pattern typical of healthy eyes, indicating the formation of a pseudofovea.³³ The eye movement map also shows visitations outlining the extent of nonfunctional fovea, which corresponds to the size and shape of the hole identified in the fundus examination. This case provides functional support to Curcio et al's^{11,12} structural findings and suggests that the visual acuity function peak corresponding to the foveola ($\approx 150 \mu\text{m}$) is most likely a result of its visual cortex representation, which is magnified at a ratio of 7:1.¹⁰

Case 5

Case 5 received bilateral accidental exposures from a Q-switched Nd:YAG laser designator, which emitted 10 laser pulses per second at a wavelength of 1,064 nm. The exit beam diameter (10 cm) was large enough to permit a simultaneous bilateral exposure. Eye position at exposure was a few centimeters from the exit aperture, with a received TIE estimated at 315 μJ per pulse. The exposure induced confined bilateral macular hemorrhages. The hemorrhage was slightly larger in OD and centered on the fovea. The patient was treated within 6 hours postexposure with a moderate steroid dose, and a taper continued for a postexposure period of 2 weeks.²³ This case will describe sequelae in the OD.

Figure 5-18 shows the laser designator and a reconstruction of the bilateral exposure scenario. At 4 days postexposure, OCT imaging showed a fovea with a break in RPE integrity beneath the fovea. At

1 month, the RPE break resolved to minimal foveal thickness. Foveal thickness at 4 months showed significant thickening close to the normal foveal thickness, and was accompanied by a return of normal color discrimination, visual acuity, and contrast

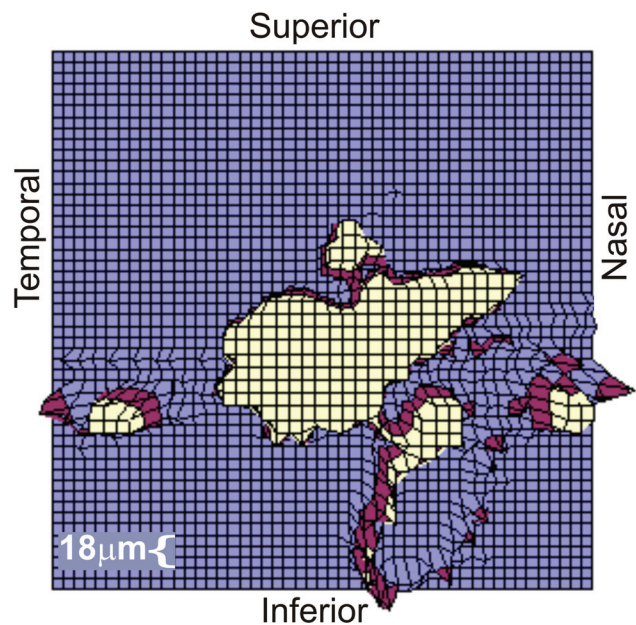


Fig. 5-17. Fixation eye movements recorded at 4 years post-exposure for fine-resolution targets. The pattern confirms the earlier finding with CSLO showing, in relation to the fovea, a superior/temporal fixation locus. Other than the shift in locus and visitation along the boundary of the hole, the fixation pattern is typical of those seen in healthy eyes. Illustration: Courtesy of the Laser Laboratory, with the technical assistance of André Akers.

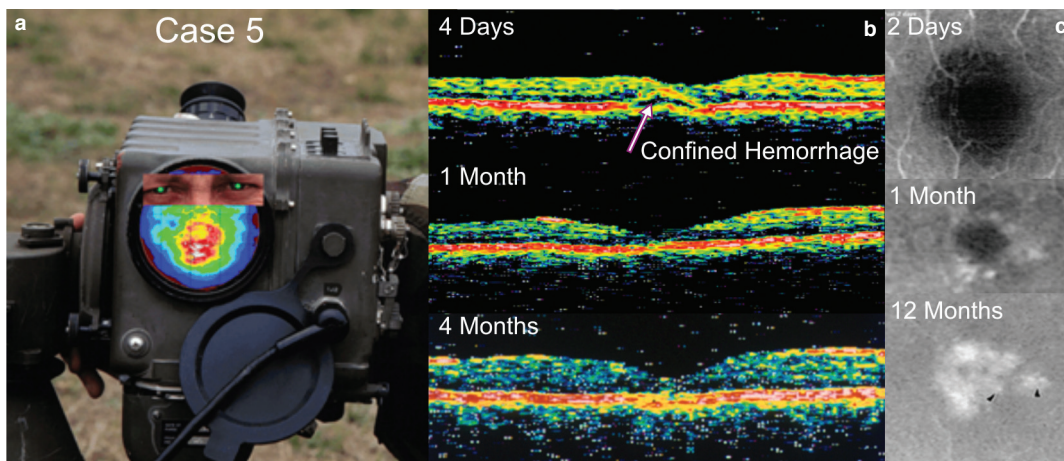


Fig. 5-18. The large exit port of the designator makes it possible for bilateral exposure at ocular distances of a few centimeters (a). OCT images (b) show the progression of OD wound healing from 4 days through 4 months, and CSLO images (c) from 2 days through 12 months postexposure.

Photographs: Courtesy of the Laser Laboratory, with the technical assistance of André Akers.

sensitivity within this same 4-month time frame. In the third column of images, corresponding CSLO images are shown revealing a reduction in the lesion size from 2 days to 1 month, and the disappearance of an ophthalmoscopically visible lesion by 12 months postexposure.¹⁶

Visual acuity at 3 hours postexposure was 20/50 OD and diminished to 20/200 OD by 2 days postexposure. Visual acuity recovered to normal levels within 3 months postexposure. Color discrimination was nominally beyond normal limits at 2 days postexposure. At 1 month postexposure, color discrimination functions were within normal limits, as measured with the FM 100 Hue examination.¹⁶ Landolt ring contrast sensitiv-

ity functions measured under CSLO visualization at 4 days postexposure showed uniform suppression, with peak sensitivity shifted from the typical 6 cycles/degree midspatial frequency peak to a peak at 1 cycle/degree. The peak shift to lower spatial frequencies indicates a disruption in foveal function. At 9 months, contrast sensitivity functions were within normal limits and corresponded to a shift in preferred retinal location (PRL) from fixation superior and slightly temporal to the fovea to within the fovea (Figure 5-19a). Figure 5-19b shows that fixation eye movements at 9 months are consistent with typical human fixation eye movement patterns.²⁴ The map shows no functional disruption within the foveal region.

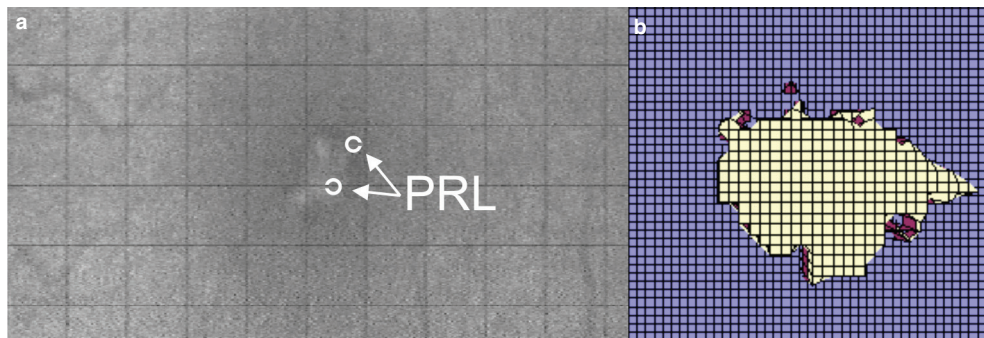


Fig. 5-19. The CSLO image shows the shift in preferred retinal location (PRL) for placing fine-resolution targets (<10 cycles/degree) from a focus superior/temporal to the fovea to a focus within the fovea (a). With the PRL return to the fovea, the fixation eye movement map (b) shows a typical pattern with no indication of residual functional damage.

Photograph/Illustration: Courtesy of the Laser Laboratory, with the technical assistance of André Akers.

REVIEW

Five laser injury cases, which involved retinal hemorrhage, were evaluated with ophthalmic techniques, which related structural insult to visual function. The results from these cases indicate the complexity of the structure–function relationship and the scope of resilience of the visual system (Table 5-1). Thus, despite similarities in dose, placement of the lesion on the retina contributed significantly to visual function outcome, but not in a classically expected manner. For example, cases 4 and 5 demonstrate that foveal damage does not equate to diminished visual acuity in that foveal-like function can be recovered through a shift in PRL from the fovea to a position superior and slightly temporal to the fovea.

Structural damage was detailed through the utilization of CSLO and OCT imaging techniques that demonstrated the depth of IRSF and RNFL-PMB damage *in vivo*, confirming previous NHP histological studies of these secondary damage processes.³⁰ CSLO imaging of retinal traction demonstrated that retinal traction exists above the RNFL and may often extend into the vitreous, possibly altering normal photoreceptor orientation, which has been demonstrated to cause reduction in visual sensitivity.³⁴

Spatial visual function metrics of visual acuity and contrast sensitivity are seriously affected by retinal traction and IRSF. These damage mechanisms alter receptor orientation of large retinal areas, reduce retinal thickness, and induce neural disorganization in the process of their formation. Case 1 showed the most serious example of traction and IRSF effects on spatial vision metrics, affecting both stationary and dynamic measures of contrast sensitivity associated with the global effects of IRSF and traction. The failure of acuity to recovery over the 2-year period is also significant, because acuity is highly “protected” by cortical magnification of the fovea relative to the parafoveal region and by findings that indicate neural receptor field plasticity or expansion that provides added neural redundancy for reduced foveal retinal neural output.³⁵

The mechanism that prevents neural plasticity in case 2 is associated with the interruption in the PMB region of the RNFL caused by induction of the paramacular hole that formed following resolution of vitreous hemorrhage. Evidence that the fovea was still functional, but could not transmit its spatial and chromatic neural output to higher order visual brain systems, was supported by fixation eye movement maps demonstrating foveal visitation capability. Although this lesion was parafoveal, and ordinarily such lesions are given less importance than more central retinal lesions, this particular lesion interrupted the

major neural pathway carrying foveal neural retinal code to higher order brain mechanism.

In the absence of secondary damage mechanisms described previously, spatial and chromatic vision may recover, but still require about 3 to 6 months to demonstrate such recovery, as seen in cases 4 and 5. The surprising release of traction in case 3 and the ensuing full recovery of color discrimination and near complete recovery of visual acuity were unexpected, but documented by the capability of CSLO imaging to capture anterior retinal pathology. Nevertheless, whereas acuity continued to recover, presumably via cortical neural compensation for reduced foveal receptor output, contrast sensitivity remained constant showing a consistent deficit in the high-spatial frequencies, which is indicative of this metric’s strong association with lower order retinal ganglion cell systems.^{36,37} On the other hand, the rapid recovery of color discrimination at 12 months to normal levels may relate to the fact that color vision photoreceptor systems are distributed over broader regions within the fovea, where photoreceptor to ganglion cell ratios are larger than those in the central fovea.

A critical factor in understanding the mechanism of neural plasticity in case 4 is the observation made with the OCT that showed a “break” in the central foveal region. This break may have caused some degree of failure in normal foveal function, resulting in a degree of dysfunction in spatial vision and PRL replacement neural mechanisms. Evidence for this hypothesis was observed in both the development of a new PRL superior and slightly temporal to the fovea and in the fixation eye movements for fine-resolution targets as mapped with the dual Purkinje eye tracker. The latter confirmed the establishment of a new PRL and further showed optical accommodation with this shift of about .25 diopters, sufficient to produce a baseline acceptable point spread function.³¹

Case 5 initially showed a PRL superior and slightly temporal to the fovea, identical to that of case 4. However, during this time, other visual functions—including visual acuity and sine wave contrast sensitivity—were still recovering through the 3 to 6 months postexposure period. During this recovery period, CSLO Landolt ring contrast sensitivity showed frequent, but not sustained, placement of Landolt ring contrast sensitivity targets within the fovea, prognostic of the recovery of foveal function. This function did recover between 6 and 9 months postexposure. Color discrimination measured with the FM 100 Hue examination had recovered in both eyes within the first month postexposure, indicating that cone mechanisms had recov-

TABLE 5-1
SUMMARY OF CASE FINDINGS

Case No.	Dose TIE (mj)	Injury Initial	Hemorrhage	Visual Acuity Initial	Visual Acuity Resultant	Contrast Sensitivity Resultant	Color Discrimination Resultant	Ocular Motor	Secondary Sequelae
1	1.96	4 Paramacular retinal lesions, 2 producing macular holes	2 Paramacular holes produced vitreous hemorrhage	20/400	20/400	Significant overall suppression peak shift to 10 cycles/degree	Overall disruption, blue axis prominence	Some functional central retinal in vicinity of scar	Retinal scar between paramacular holes bridging the macular and associated traction
2	1.0	Full-thickness paramacular hole, temporal to optic disc, nasal to macular in PMB	Vitreous hemorrhage	20/50	20/800	Not measurable beyond 6 cycles/degree	Uniform suppression with no dominant axis	Atypical vertical scan pattern with no dominant retinal site attracting eye movement	Considerable nerve fiber degeneration in PMB with evidence of Wallerian degeneration to the optic nerve
3	2.5-3.0	Full-thickness 100-µm diameter central macular hole	Vitreous hemorrhage	20/150	20/40	Significant suppression in OD sensitivity from 6 to 30 cycles/degree	WNL	Significant typical horizontal scan with persistence of atypical vertical component	Reduction in hole size and disappearance of traction bands
4	1.0	Small flat macular hole through the center of the fovea	Vitreous hemorrhage	20/200	20/15	Contrast sensitivity function within normal limits, although at the lower normal limit	WNL	PRL superior/temporal to fovea with typical fixation movement pattern	No change from initial injury
5	0.315	Break in RPE beneath the fovea	Confined macular hemorrhage centered in fovea	20/50 OD at 3 hours, 20/200 at 2 days postexposure	20/15 OU at 10 months and 20/25 OU at 14 months (OD only was not recorded)	Recovered from uniform suppression with peak sensitivity shifted to 1 cycle/degree to a function within normal limits	WNL	PRL shift from superior/temporal to fovea back to the fovea	Treated with steroid, significant nerve fiber thickening close to normal, foveal thickness

OD: oculus dexter (pertains to the right eye); OU: oculus uterque (pertains to both eyes); PMB: papillomacular bundle; PRL: preferred retinal location; RPE: retinal pigmented epithelium; TIE: total intraocular energy; WNL: within normal limits.

EXHIBIT 5-3

THE FUTURE AND FUTURE RESEARCH

The emergence of the use of military systems that emit hazardous levels of electromagnetic radiation continues. Few eye injuries in Operation Iraqi Freedom (OIF) and Operation Enduring Freedom (OEF) current operations have been attributed to laser radiation. However, laser range finders, designators, illuminators, training devices, retinal scanned displays, high-energy laser systems for both tactical and theater ballistic missile defense, secure infrared communication systems, laser battlefield contaminant detection systems, and laser “dazzlers” all present new threats to soldier health and performance.

Optical denial systems use radiation in the optical region of the electromagnetic spectrum. Laser dazzlers, such as HELIOS and GHOST (developed by the US Army’s Rapid Equipping Force), emerged in 2006 for rapid insertion into OIF and OEF operations. The emergence of a solid-state fiber laser with emission powers in the 25–100 kW range in a relatively small package has reenergized the military system developers in refining application specifications. Tactical high-energy lasers are emerging with potential injury to personnel a likely scenario in both training and operational scenarios. The maturing of access denial systems that operate in the infrared and millimeter wavelength regions requires enhanced awareness of the medical effects by the Army Medical Department. Issues with respect to their testing, training, and fielding will require judgment from the Army Medical Department in the protection of soldiers. New military radar systems, individual soldier communications systems with body-worn antennas for local situational awareness, electronic countermeasures, guidance and jamming systems, satellite communications, and rail guns all use or generate radiofrequency radiation. A robust biomedical database of radiation effects pertinent to the wide range of military systems is required to protect the soldier and to sustain military operations.

Treatment of laser-induced retina injury must continue to be a focal area of research to minimize the loss of vision induced by laser radiation for a wide range of exposure conditions inherent to the multiplicity of military uses of directed energy. Whereas the relative efficacy of some drugs has been demonstrated for specific forms of laser-induced injury, combined therapies and possible stem cell applications will offer better treatment efficacy. Eye injuries from blast and fragments are a problem in current operations. Pharmacological and surgical interventions under investigation for laser-induced retinal trauma certainly have applicability to eye trauma from blast. Local as opposed to systemic administration of drugs to the eye requires testing of innovative approaches. Ocular pharmacokinetics and optical techniques to make both qualitative and quantitative assessments are required for treatment of ocular trauma.

The medical aspects of laser exposure from glare to laser-induced hemorrhage must be better understood. Evaluation of laser accident cases has demonstrated changes in the retina occurring over a year postinjury. Long-term follow-up of these cases should be continued. Definition of the degree and time course of visual impairment inherent to battlefield laser exposure requires additional research. With the emergence of visible laser dazzlers, the issue of long-term effects from repeated exposure (several focal “full bleach” exposures with no ophthalmoscopically observable changes) in a single, multiple exposure engagement or cumulative effects over a period of days or months are not well characterized or understood. Developments of advanced rapid assessments of visual function are needed to ensure the soldiers’ visual health in operational scenarios and to have early assessment of potential functional changes from repeated or chronic exposure. Advanced diagnostic imaging of the retina (optical coherence tomography, scanning laser ophthalmoscopy, wave front-corrected retinal imaging) have great potential in assisting far-forward ocular evaluations, particularly when coupled to telemedicine implementations. Medical research programs must be focused and sustained to provide better triage and treatment solutions for the future. Interim triage and treatment protocols must be established now. Exploration of the efficacy of new drugs and the combination of drugs are based on the mechanism of injury at the molecular level, and the subsequent time course and manifestation of the injury pathway.

The biological database that supports development of exposure guidelines for lasers must continue to be expanded to meet the challenges posed by new military systems. With the emergence of nonlethal-directed energy systems, soldier protection must be ensured by the availability of “results-based” directed energy exposure guidelines. This database must also assist in the specification of the level of protection required for laser eye protection systems.

A closer cooperation with military laser developers is needed to ensure that the system technology does not exceed the understanding of the biomedical implications of soldier exposure. The emergence of nonlethal-directed energy will require updates to testing and training policies for soldier exposure to nonionizing radiation. New technology must be used to assess radiation bioeffects, to understand injury mechanisms, and to determine the efficacy of treatment regimens. As the research in the use of these technologies matures, the results must be integrated in military medical doctrine and practice.

ered or were sufficiently active to minimize possible residual selective cone dysfunction. This is most likely due to a greater inherent redundancy of the cone-to-ganglion cell ratio in the foveal regions and further magnification of this relationship to the visual cortex.

At nonhemorrhagic levels, metrics that evaluate outer retinal cone system functionality appear to be more sensitive than those that rely on achromatic metrics of visual acuity and not on contrast sensitivity.¹⁸ However, when accidental exposure is repeated by malfunction¹⁹ or by intentional exposure,³⁶ functional loss in spatial retinal-based metrics may become permanent, although high-contrast achromatic visual acuity may still be compensated by static or dynamic visual cortex plasticity. Of special note is the color contrast examination developed by Arden et al¹⁹ that uses both color opponency and color contrast. These metrics interrogate both retinal ganglion cells, as well as higher order visual processing that render contrast, color opponency, and color contrast information. Although this test represents a major advance in utilizing various levels of neural code arising from the retina, it could be improved to track the neural code arising from the fovea as well, by utilizing a broader range of spatial frequencies in evaluation of retinal systems associated with central fovea visual function. This is the current effort for the enhancement of the Aidman Vision Screener.²²

Finally, the animal behavioral and morphological evaluations of outer retinal cone function require some discussion. Sperling et al³⁸ demonstrated the photic toxicity of short wavelength light to S cone photoreceptors and that such exposures occurred in the range of 5 log trolands. This brightness level is slightly higher than comfortable brightness, but is not considered a thermal threat. However, prolonged exposure to such levels of highly monochromatic blue light did produce permanent deficits in S cone incremental spectral sensitivity, indicating that either the S cone or some other component in the retina sensitive to such visible radiation was vulnerable.³⁹ The experiments of Zwick² and Schmeisser⁴⁰ bring another aspect to this discussion, which is the possibility that the unique interference patterns induced by visible laser light when irradiating a surface (speckle) may have peak powers high enough to produce significant retinal dysfunction or photoreceptor loss. Although this hypothesis remains to be validated, it should be pointed out that higher order brain mechanisms continue to form complex methods of producing images from unique neural signals, and prolonged viewing of speckle with moderate peak powers above average power may induce neural reorganization in ways that may degrade visual function. Notwithstanding, parallel exposures made on NHPs revealed unique histopathological find-

ings of increases in basal bodies and striated rootlets within the RPE that indicate significant physiological changes can be induced by such exposure.⁴¹ These changes may have been responsible for detuning receptor systems associated with high acuity criteria and sensitizing receptor systems at lower acuity criteria; but, over about a 2-year period, receptor systems appear to have been reorganized with peaks and levels of sensitivity consistent with those of higher acuity spectral sensitivity functions. These observations are consistent with similar long wavelength cone system emergence following acute foveal injury to small spot Q-switched 690 nm dye laser exposure,² suggesting that such effects may be triggered by a wide range of laser energy exposure levels.

The ability to address the diagnostic issues reviewed herein with an animal model capable of providing an *in vivo* view of such processes in "action" is unique. The authors have shown, in imaging damage and repair processes in the small eye, changes in the internal reflection of the photoreceptor indicative of changes in mode structure.⁴² Changes in mode structure suggest a change in photoreceptor orientation and thus in sensitivity to particular spectral frequencies.⁴³ Such reflectivity is not the same as a lesion observed in a large eye (eg, NHP) due to the full thickness and low resolution with respect to cellular structure in the large eye. The *in vivo* small eye model is different from histological preparations, as well, because it exists in its natural state within the retina and its behavior can be documented, such as changes in orientation, reflectivity, and migration into the center of a laser retinal injury site. The latter has been suggested as a retinal plasticity mechanism and documented by retinal photoreceptor histology, suggesting that, over time, peripheral photoreceptors may migrate into lesion sites clear of damaged photoreceptors.⁴⁴ The importance of this observation relates to the fact that, in the NHP and human retina, damaged photoreceptors in the fovea are dominated by cones. Therefore, replacement receptors from peripheral retina, if migration is a relevant explanation of visual function recovery, must have characteristics that provide trichromatic cone characteristics. Such characteristics may simply be the greater redundancy that worked in case 5 for return of color discrimination. However, long wavelength cone emergence was also demonstrated over very different spectral and energy levels, suggesting that the reemergence of long wavelength cone systems may involve unique photoreceptor spectral tuning requiring an active rootlet system within the photoreceptor, as well as one within the RPE to provide a range of movement parameters that might be necessary for such spectral tuning of the waveguide (Exhibit 5-3).⁴⁵

SUMMARY

The wide variety of damage and recovery processes was revealed through metrics that combine structural and functional diagnostic techniques. The techniques are needed for reliable, rapid, and valid measures of visual function deficits associated with laser retinal injury and will require further development as lasers become smaller, more spectrally agile, and more widespread. In the military situation, rapid differential diagnostic procedures are required to identify laser-induced retinal injury. These procedures will require compact ophthalmoscopes with axial, as well as transverse, retinal imaging capability with integrated visual function tests that interrogate the span of visual processing from the retina into higher order vi-

sual centers. This investigative functionality will allow for the identification of vision loss without easily identifiable retinal damage, because a dysfunctional state may exist within the retinal/brain physiology itself.

As adjunct to other military systems, and possibly as weapons in their own right, lasers will continue to play an important and sometimes dangerous role on the modern battlefield. At present, there is no adequate comprehensive protection against accidental or intentional exposure to lasers in combat. Thus, it is critical that the field of laser safety research move forward toward the development of preventative protocols and prophylactic technologies to protect military personnel and to support military operational objectives.

Acknowledgment

The authors thank Dr Victoria Tepe for her invaluable assistance in preparing this manuscript and an extract of a previous work on Biomedical Implications of Military Laser Exposure (SURVIAC [Survivability/Vulnerability Information Analysis Center] Technical Report for the US Army Medical Research Detachment, Medical Research and Materiel Command, 2007).

REFERENCES

1. Wolfe JA. Laser retinal injury. *Mil Med.* 1985;150:177–185.
2. Zwick H. Visual functional changes associated with low-level light effects. *Health Phys.* 1989;56:657–663.
3. Barkana Y, Belkin M. Laser eye injuries. *Surv Ophthalmol.* 2000;44:459–478.
4. Masters B, Boenke M. Three-dimensional confocal microscopy of the living human eye. *Ann Rev Biomed Eng.* 2002;4:69–91.
5. Zwick H, Elliot R, Schuschereba S, et al. In-vivo confocal scanning laser ophthalmoscopic characterization of retinal pathology in a small-eye-animal model. *Proc SPIE.* 1997;2974:44–50.
6. Zwick H, Elliot R, Li G, et al. In-vivo imaging of photoreceptor structure and laser injury pathophysiology in the snake eye. *Proc SPIE.* 1999;359:368–374.
7. Li G, Zwick H, Tribble J, et al. On-off-axis confocal double pass measurements of the point spread function in the human eye. *Proc SPIE.* 1999;3591:351–358.
8. McIlwain J. *An Introduction to the Biology of Vision.* New York, NY: Cambridge University Press; 1996.
9. Brodal P. *The Central Nervous System: Structure and Function.* 3rd ed. New York, NY: Oxford University Press, Inc.; 2004.
10. Langus A, Zwick H, Stuck B, Belkin M. Foveal photoreceptor explanation of short-term visual acuity recovery associated with laser-induced foveal damage. *Proc SPIE.* 2003;4953:39–50.
11. Curcio CA, Kimberly AA, Sloan KR, et al. Distribution and morphology of human cone photoreceptors stained with anti-blue opsin. *J Comp Neurol.* 1991;312:610–624.
12. Curcio C, Allen K. Topography of ganglion cells in human retina. *J Comp Neurol.* 1990;300:5–25.

13. Zwick H, Stuck B, Dunlap W, et al. Accidental bilateral Q-switched neodymium laser exposure: treatment and recovery of visual function. *SPIE*. 1998;3254:80–89.
14. Breitmeyer B, Valberg A. Local foveal inhibitory effects of global peripheral excitation. *Science*. 1979;203:463–464.
15. Allen D. Fourier analysis and the Farnsworth-Munsell 100-Hue test. *Ophthalmic Physiol Opt*. 1985;5:337–342.
16. Zwick H, Lund B, Brown J, et al. Human color vision deficits induced by accidental laser exposure and potential for long-term recovery. *Proc SPIE*. 2003;4953:27–39.
17. Zwick H, Bedell RB, Bloom KR. Spectral and visual deficits associated with laser irradiation. *Mod Probl Ophthalmol*. 1974;13:299–306.
18. Zwick H, Bloom KR, Beatrice ES. *Permanent Visual Change Associated with Punctate Foveal Lesions*. Presidio of San Francisco, Calif: Letterman Army Institute of Research; 1986. Institute Report No. 86-59.
19. Arden GB, Grundez K, Perry S. Colour vision testing with a computer graphics system. *Clin Vis Sci*. 1988;2:303–320.
20. Rabin J. Cone specific measures of human color vision. *Invest Ophthalmol Vis Sci*. 1996;37:2771–2774.
21. Gunzenhauser J. *Issues in the Development of the Aidman Vision Screener*. Laboratory Report. Presidio of San Francisco, Calif: Letterman Army Institute of Research; 1990.
22. Boye M, Zwick H, Stuck B, et al. Development of an Advanced Aidman Vision Screener (AVS) for selective assessment of outer and inner laser-induced retinal injury. *Proc SPIE*. 2007;6426:2–10.
23. Zwick H, Stuck B, Brown J, et al. Long term evaluation of two bilateral laser eye accident cases. *Proc Intl Laser Safety Conf*. 1999;83–92.
24. Ness J, Zwick H, Stuck B, et al. Retinal image motion during deliberate fixation: implications to laser safety for long duration viewing. *Health Phys*. 2000;78:131–142.
25. Zwick H, Stuck B, Gagliano D, et al. *Two Informative Cases of q-Switched Laser Eye-Injury*. Presidio of San Francisco, Calif: Letterman Army Institute of Research; 1991. Institute Report No. 463.
26. Stuck B, Zwick H, Molchany J, et al. Accidental human laser retinal injuries from military laser systems. *SPIE*. 1996;2674:7–20.
27. Robson JG. Spatial and temporal contrast sensitivity functions of the human visual system. *J Opt Soc Am A Opt Image Sci Vis*. 1996;56:1141–1142.
28. Chatterjee S, Callaway E. S cone contributions to the magnocellular visual pathway in the macaque monkey. *Neuron*. 2002;35:1135–1146.
29. Frisch G, Shawaluk P, Adams D. Remote nerve fibre bundle alterations in the retina caused by argon laser photocoagulation. *Nature*. 1974;248:433–435.
30. Zwick H, Belkin M, Zuclich J, et al. Laser-induced retinal nerve fiber layer injury in the nonhuman primate. *Proc SPIE*. 1996;2674:89–96.
31. Ness J, Zwick H, Lund B, et al. Fixational eye movement patterns reflect macular pathology induced by accidental laser exposure. *Invest Ophthalmol Vis Sci*. 2000;41(4). Abstract 4323-B270.
32. Zwick H, Stuck B, Scales D, et al. Longitudinal evaluation of selected human laser eye accident cases. Laser and non-coherent light ocular effects: epidemiology, prevention and treatment. *Proc SPIE*. 1999;3591:386–393.

33. Zwick H, Ness J, Molchany J, et al. Neural motor ocular strategies associated with the development of a pseudo-fovea following laser-induced macular damage and artificial macular occlusion: is the fovea replaceable? *J Laser Appl.* 1998;10:144–147.
34. Enoch J, Van Loo J, Okun E. Realignment of photoreceptors disturbed in orientation secondary to retinal detachment. *Invest Ophthalmol Vis Sci.* 1973;12:849–853.
35. Gilbert C, Wiesel T. Receptive field dynamics in adult primary visual cortex. *Nature.* 1992;356:150–152.
36. Jenkin M, Harris L. *Seeing Spatial Form.* New York, NY: Oxford University Press; 2006.
37. Robbins DO, Zwick H. Subthreshold functional additivity occurring at the transition zone between temporary and permanent laser-induced visual loss. *Proc SPIE.* 1996;2674:44.
38. Sperling HG, Johnson C, Harwerth RS. Differential spectral photic damage to primate cones. *Vision Res.* 1980;20:1117–1125.
39. Ham WT Jr, Mueller HA, Sliney DH. Retinal sensitivity to damage from short wavelength light. *Nature.* 1976;11:153–155.
40. Schmeisser E. Laser flash effects on laser speckle shift VEP. *Am J Optom Physiol Opt.* 1985;62:709–714.
41. Schuschereba S, Zwick H, Stuck B, Beatrice E. *Basal Body and Striated Rootlet Changes in Primate Macular Retinal Pigmented Epithelium After Low Level Diffuse Argon Laser Radiation.* Fort Belvoir, Va: Defense Technical Information Center; 1982.
42. Zwick H, Edsall P, Stuck B, et al. Laser-induced photoreceptor damage and recovery in the high numerical aperture eye of the garter snake. *Vision Res.* 2008;48:486–493.
43. Li G, Zwick H, Stuck B, Lund D. On the use of schematic eye models to estimate image quality. *J Biomed Opt.* 2000;5:307–314.
44. Tso MO, Robbins DO, Zimmerman LE. Photic maculopathy. A study of functional and pathologic correlation. *Mod Probl Ophthalmol.* 1974;4:220–228.
45. Westheimer G. Directional sensitivity of the retina: 75 years of Stiles-Crawford effect. *Proc R Soc Biol Sci.* 2008;275:2777–2786.

